

Dynamics and universality in noise-driven dissipative systemsEmanuele G. Dalla Torre,^{1,2} Eugene Demler,² Thierry Giamarchi,³ and Ehud Altman¹¹*Department of Condensed Matter Physics, Weizmann Institute of Science, Rehovot 76100, Israel*²*Department of Physics, Harvard University, Cambridge, Massachusetts 02138, USA*³*DPMC-MaNEP, University of Geneva, 24 Quai Ernest-Ansermet, 1211 Geneva, Switzerland*

(Received 17 October 2011; published 10 May 2012)

We investigate the dynamical properties of low-dimensional systems, driven by external noise sources. Specifically we consider a resistively shunted Josephson junction and a one-dimensional quantum liquid in a commensurate lattice potential, subject to $1/f$ noise. In absence of nonlinear coupling, we have shown previously that these systems establish a nonequilibrium critical steady state [Dalla Torre, Demler, Giamarchi, and Altman, *Nat. Phys.* **6**, 806 (2010)]. Here, we use this state as the basis for a controlled renormalization group analysis using the Keldysh path integral formulation to treat the nonlinearities: the Josephson coupling and the commensurate lattice. The analysis to first order in the coupling constant indicates transitions between superconducting and localized regimes that are smoothly connected to the respective equilibrium transitions. However, at second order, the back action of the mode coupling on the critical state leads to renormalization of dissipation and emergence of an effective temperature. In the Josephson junction, the temperature is parametrically small allowing to observe a universal crossover between the superconducting and insulating regimes. The I - V characteristics of the junction displays algebraic behavior controlled by the underlying critical state over a wide range. In the noisy one-dimensional liquid, the generated dissipation and effective temperature are not small as in the junction. We find a crossover between a quasilocalized regime dominated by dissipation and another dominated by temperature. However, since in the thermal regime the thermalization rate is parametrically small, signatures of the nonequilibrium critical state may be seen in transient dynamics.

DOI: [10.1103/PhysRevB.85.184302](https://doi.org/10.1103/PhysRevB.85.184302)

PACS number(s): 05.70.Ln, 37.10.Jk, 71.10.Pm, 03.75.Kk

I. INTRODUCTION

Advances in the fabrication and coherent manipulation of quantum many-body systems, such as mesoscopic devices, superconducting circuits,^{1–3} and ultracold atomic gases,⁴ allow to investigate new regimes of many-body physics and open the way to interesting technological applications. A recurring issue with these systems is that they are often being driven out of equilibrium, either purposely as part of the preparation scheme, or due to their sensitivity to external noise sources. Such studies provide a strong motivation for understanding the properties of quantum many-body systems under nonequilibrium conditions (see, e.g., Refs. 5 and 6). Since a full microscopic description of such complex systems is, in general, hopeless, it is important to identify regimes where the complexity of the dynamics gives rise to robust emergent behavior that is independent on the microscopic details.

In this paper, we describe universal quantum phenomena that occur in many-body systems subject to external noise sources that are not in thermal contact with the system. We have previously identified a class of quantum-critical steady states that arise under these conditions.⁷ Specifically, we considered quadratic model systems, such as quantum RC circuits and Luttinger liquids at zero temperature subject to $1/f$ noise. Clearly, the correlation and response of the systems are modified by the noise and show manifestly nonequilibrium phenomena. But, as we showed, the scale invariance and hence the algebraic decay of the correlations is not destroyed. Nonlinear perturbations such as a Josephson junction in the RC circuit or a commensurate periodic potential in the Luttinger liquid were considered using simple scaling arguments. This analysis showed that the perturbations can be tuned from being relevant to irrelevant by

varying the noise power, suggesting a possible nonequilibrium phase transition. The key issue that was not addressed by the simple scaling arguments is the back action of the nonlinear perturbations on the quadratic elements of the system.

Here, we extend our previous analysis and use the critical steady states as a starting point for a perturbative real-time renormalization-group (RG) approach. This method was used in Ref. 8 to describe a quench of a Luttinger liquid in a commensurate periodic potential. In the quench problem,^{8,9} the mode-coupling induced by the lattice potential led to the generation of finite dissipation and temperature. In the present paper, we generalize the RG scheme and extend it to our case of interest, namely, the steady-state regime of quantum systems subjected to $1/f$ noise. This allows us to study the effects of small perturbations around the “nonequilibrium quantum critical points” in a controlled way. The first-order expansion agrees with the predictions made in Ref. 7 by means of the scaling argument. However, the second order shows the appearance of new physics, which was hidden by the trivial scaling analysis.

We highlight the new effects in the example of a “zero-dimensional” noisy Josephson junction for which we obtain the full dynamical phase diagram. For such a system, temperature and friction are generated by the combination of the out of equilibrium noise and the mode coupling terms. The emergent effective temperature acts to smear out the quantum phase transition predicted in Ref. 7. However, unlike the case of equilibrium thermal noise, the universal crossover is governed by the nonequilibrium quantum critical line. At distances smaller than the effective thermal length, the critical correlations explicitly violate the equilibrium fluctuations-dissipation theorem (FDT).

By the present method, we also analyze the noisy one-dimensional system of interacting particles. Interestingly, although the microscopic starting point is quite different from the case of quenched systems, the initial steps of the flow are similar to Refs. 8 and 9.

The plan of the paper is as follows: the paper starts in Sec. II with a definition of the models that we consider, namely, the noisy Josephson junction and the noisy 1D Luttinger liquid. Section III, offers a self-contained description of our general RG framework. This section can be safely skipped by the reader mostly interested in the results and not in the actual method used to obtain them. Such results are discussed in the next two sections. Section IV discusses the case of the noisy Josephson junction. In particular, the dynamical phase diagram and its physical implications have been regrouped in Secs. IV C and IV D. In a similar way, the noisy 1D chain is examined in Sec. V, with the physical results in Sec. V B. Section VI closes the article with a summary of our results and an outline of future research directions.

II. MODELS

Below we describe the specific models of the noisy Josephson junction and the noisy Luttinger liquid considered in this paper. Both systems consist of three key elements: (i) a quantum system of interacting particles, described by a many-body Hamiltonian H_{sys} , (ii) a deterministic noise source, described by a stochastic time-dependent Hamiltonian $H_{\text{noise}}(t)$, and (iii) a dissipative quantum bath H_{bath} . In what follows, we will assume that the dissipative bath is initially prepared at equilibrium, and due to its large size, does not significantly deviate from this state throughout the whole experiment. Considering only noise averaged quantities, we then obtain a steady state in which correlation and response functions depend only on the time difference. Due to the constant flow of energy through the system, from the noise source to the zero temperature bath, these correlations and the response function explicitly violate the equilibrium fluctuation-dissipation theorem (FDT) and are derived in the framework of a nonequilibrium Keldysh action that will be described below. For a classical analogue to this problem see for example Ref. 10 Bonart *et al.*

A. Noisy shunted Josephson junction

The first system that we consider here is the resistively shunted Josephson junction driven by $1/f$ charge noise. This model is defined by the time-dependent Hamiltonian

$$H(t) = E_J \cos(\theta) + E_c \left[n - \frac{Q(t)}{2e} \right]^2 + H_{\text{bath}}(n). \quad (1)$$

Here, θ is the phase difference across the junction and n its canonical conjugate (the charge). $E_c = 2e^2/C$ and $E_J = \hbar g$ are, respectively, the charging energy and the Josephson coupling of the junction. $Q(t)$ describes the stochastic time-dependent fluctuations of the off-set charge of the junction (charge noise).^{11–14} H_{bath} models the resistor in terms of an infinite set of harmonic oscillators.^{15,16} The model can also be represented by the electric circuit of Fig. 1 in which the charge noise is generated by a fluctuating voltage source $V_n(t) = CQ(t)$.

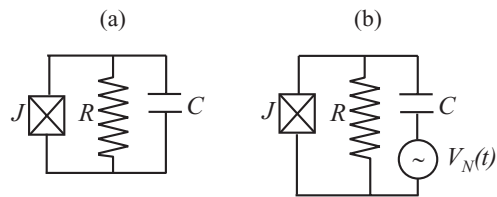


FIG. 1. Electric circuit of a resistively shunted Josephson junction (1). (a) The junction is at equilibrium. (b) The junction is driven out of the equilibrium by time-dependent charge noise, modeled by a stochastic voltage source $V_n(t) = CQ(t)$.

Assuming a Gaussian distribution, we average over the noise and obtain an effective action⁷ that can be written in the Keldysh form:

$$\begin{aligned} S &= S_{\text{bath}} + S_{\text{noise}} + S_g, \\ S_{\text{bath}} &= \int \frac{d\omega}{2\pi} (\theta_\omega^* \hat{\theta}_\omega^*) G_{\text{bath}}^{-1} \begin{pmatrix} \theta_\omega \\ \hat{\theta}_\omega \end{pmatrix}, \\ S_{\text{noise}} &= \int \frac{d\omega}{2\pi} (\theta_\omega^* \hat{\theta}_\omega^*) G_{\text{noise}}^{-1} \begin{pmatrix} \theta_\omega \\ \hat{\theta}_\omega \end{pmatrix}, \\ S_g &= g \int dt \sin(\theta) \sin(\hat{\theta}). \end{aligned} \quad (2)$$

Here, θ and $\hat{\theta}$ are the symmetric and antisymmetric combinations of the forward (θ_+) and backward (θ_-) paths: $\theta_\pm = \theta \pm \hat{\theta}$. An introduction to Keldysh path integrals see, for example, Ref. 17. The two fields θ and $\hat{\theta}$ are, respectively, referred to as the “classical” and “quantum” fields.

The inverse Green’s function of the bath is

$$G_{\text{bath}}^{-1} = \begin{pmatrix} 0 & R_Q C \omega^2 - i \frac{R_Q}{R} \omega \\ R_Q C \omega^2 + i \frac{R_Q}{R} \omega & -2i \frac{R_Q}{R} \omega \coth\left(\frac{\omega}{2T}\right) \end{pmatrix}. \quad (3)$$

Here, $R/R_Q = R[(2e)^2/h]$ and T are, respectively, the normalized resistance and the temperature. For $1/f$ charge noise, $\langle Q_\omega^* Q_\omega \rangle = (2e)^2 F/|\omega|$ and

$$G_{\text{noise}}^{-1} = \begin{pmatrix} 0 & 0 \\ 0 & -4\pi i F |\omega| \end{pmatrix}. \quad (4)$$

For later convenience, we define a scaled noise parameter

$$\bar{F} \equiv 2\pi(R/R_Q)F. \quad (5)$$

Note that the noise contributes only to the quantum-quantum part of the action; it introduces only fluctuations in the system, without any dissipation, and therefore explicitly violates the equilibrium fluctuation-dissipation theorem (FDT).

As shown in Ref. 7, $1/f$ noise preserves the scale invariance of the quadratic model. As a result, physical correlations decay as power laws in time. Of particular interest are the correlation $\mathcal{K}(t)$ and response function $\mathcal{R}(t)$ of the Cooper pair creation operator $e^{i\theta}$. These are easily calculated within the quadratic theory to be⁷

$$\begin{aligned} \mathcal{K}(t - t') &\equiv \frac{1}{2} \langle e^{i\theta_+(t')} (e^{i\theta_+(t)} + e^{i\theta_-(t)}) \rangle \\ &\approx \left(\frac{RC}{|t - t'|} \right)^{2(1+\bar{F})R/R_Q}, \end{aligned} \quad (6)$$

$$\begin{aligned} \mathcal{R}(t-t') &\equiv \frac{i}{2} \langle e^{i\theta_+(t')} (e^{i\theta_+(t)} - e^{i\theta_-(t)}) \rangle \\ &\approx \Theta(t) \sin\left(\pi \frac{R}{R_Q}\right) \mathcal{K}(t-t'). \end{aligned} \quad (7)$$

An important goal of this work is to investigate the effect of the nonlinear coupling introduced by the Josephson junction on the steady state of the system. We shall study these effects in Sec. IV using a real-time RG within the Keldysh framework. The general RG scheme is described below in Sec. III.

B. Noisy Luttinger liquid

The second example that we consider consists of interacting particles in one dimension coupled to a quantum bath and to a source of time-dependent noise. The many-body Hamiltonian describing the system, the bath, and the noise is

$$\begin{aligned} H(t) &= \frac{1}{2\pi} \int \frac{dx}{u} \left\{ K [u\pi \partial_x \theta(x)]^2 \right. \\ &\quad \left. + \frac{1}{K} [u\partial_x \phi(x)]^2 - g(x) \cos(2\phi) \right\} \\ &\quad + H_{\text{bath}}(\phi) - \frac{1}{\pi} \int \frac{dx}{u} f(x,t) \partial_x \phi(x). \end{aligned} \quad (8)$$

The first two terms are the standard Luttinger liquid Hamiltonian with Luttinger parameter K and sound velocity u . The fields $\theta(x)$ and $-(1/\pi)\phi(x)$ are, respectively, the phase of the bosons and their long-wavelength density fluctuations.^{18–21} They satisfy the canonical commutation relation: $[-\frac{1}{\pi}\partial_x \phi(x), \theta(x)] = i\delta(x-x')$. The cosine term describes an external static potential. In particular, $g(x) = gu\delta(x)$ models a local impurity,²² while $g(x) = g$ models a periodic potential at commensurate filling.²³ The last two terms of Eq. (8) describe, respectively, a dissipative bath and a stochastic time-dependent noise, linearly coupled to the long-wavelength fluctuations of the density. In Ref. 7, we have discussed specific examples, such as one-dimensional systems of ultracold polar molecules and chains of trapped ions for which this model is expected to be relevant.

After averaging over the noise, we obtain the following real-time action:

$$S = \int \frac{udq}{2\pi} \frac{d\omega}{2\pi} (\phi^* \hat{\phi}^*) G_{1d}^{-1} \left(\begin{array}{c} \phi \\ \hat{\phi} \end{array} \right) + \int dt dx g(x) \cos(2\phi). \quad (9)$$

Here,

$$G_{1d}^{-1} = \left(\begin{array}{cc} 0 & \frac{1}{\pi K} (\omega^2 - u^2 q^2) + i\eta\omega \\ \frac{1}{\pi K} (\omega^2 - u^2 q^2) - i\eta\omega & -2i\eta(|\omega| + \frac{F}{\eta} \frac{q^2}{|\omega|}) \end{array} \right). \quad (10)$$

Here, we assumed a noise spectrum $F(q, \omega) = \langle f^*(q, \omega) f(q, \omega) \rangle = F/|\omega|$, implying that the noise couples to smooth density fluctuations but is uncorrelated at long scales. This behavior of the noise spectrum is consistent with recent measurements of $1/f$ noise on cold trapped ions.^{25,26} The parameter η describes the coupling strength to the bath, which is assumed to be linear, ohmic, and at zero temperature. (For the physical motivations of these assumptions, see

Supplementary Material of Ref. 7.) For later convenience, we also define the dimensionless noise strength

$$\bar{F} = \frac{F}{u^2 \pi^2 \eta}. \quad (11)$$

The model (9) is analogous to the zero-dimensional case presented above, see Eq. (2), with one important difference. In Eq. (2), the coupling to the thermal bath R/R_Q was a dimensionless parameter. Here, on the other hand, the coupling η has units of momentum and is therefore relevant in an RG sense. To access the quantum critical point, we restrict ourselves to the case of a weak coupling between the system and the bath by considering the limit of $\eta \rightarrow 0$ (while keeping a fixed \bar{F}). Our results are therefore valid only for length scales smaller than $1/\eta$. In fact, this limitation is often less restrictive than other infrared cutoffs already existing in the system, such as the finite size of the sample.

In the absence of an external potential [$g(x) \equiv 0$], the action is quadratic and one can easily compute any physical observable. Consider for instance the crystalline order parameter $O(x) = \cos[2\phi(x)]$, which measures the closeness of the system to a perfect crystal. [$O(x) = 1$ in a perfect crystal and $O(x) = 0$ in a noninteracting gas.] At equilibrium, this order parameter decays algebraically signaling a quasi-long-range ordered crystal. In the presence of the noise, we have previously shown⁷ that the crystalline order is still algebraic but with a modified exponent. Specifically, the correlation and response functions of the crystalline order are respectively given by

$$\begin{aligned} \mathcal{K}(x-x', t-t') &\equiv \frac{1}{2} \langle e^{i\phi_+(x',t')} (e^{i\phi_+(x,t)} + e^{i\phi_-(x,t)}) \rangle \\ &\approx \left[\frac{a^2}{(x-x')^2 - u^2(t-t')^2} \right]^{K(1+\bar{F})}, \quad (12) \\ \mathcal{R}(x-x', t-t') &\equiv \frac{i}{2} \langle e^{i\phi_+(x',t')} (e^{i\phi_+(x,t)} - e^{i\phi_-(x,t)}) \rangle \\ &\approx \sin(\pi K) \Theta[u(t-t') - |x-x'|] \mathcal{K}(t-t'). \end{aligned} \quad (13)$$

Here, a the interparticle distance (i.e., the natural UV cutoff). If $\bar{F} \neq 0$, we obtain a scale invariant state that explicitly violates the equilibrium fluctuation-dissipation theorem: a nonequilibrium quantum critical state. This situation is encountered, for example, at the edges of quantum Hall states²³ where, due to the chirality of the modes, back scattering is forbidden. Nonequilibrium scaling of interacting particles in 1D is also described in Refs. 27 and 28.

The static potential introduces a nonlinear mode coupling term and our goal is to understand its effect on the critical steady state described above. Let us first discuss the case of a local impurity potential, i.e., $g(x) = gu\delta(x)$. This can be thought of as a modified Kane-Fisher problem²² where the Luttinger liquid lead is subject to local $1/f$ noise. Similarly to the equilibrium case, this problem can be mapped exactly to the Josephson junction model described above. To explicitly see the mapping, we integrate out the Luttinger liquid and obtain an effective action for the field $\phi_\omega(x=0)$ on the impurity site. The

quadratic part of the action is then simply the inverse Green's function of this field calculated in the quadratic theory (10):

$$\begin{aligned}
G_K(\omega, x=0) &= i \langle \phi_\omega^*(0) \phi_\omega(0) \rangle \\
&= i \lim_{\eta \rightarrow 0} \frac{K}{2\pi} \int (udq) \frac{\eta|\omega| + \frac{Fq^2}{|\omega|}}{|u^2q^2 - \omega^2 - i\eta\omega|^2} \\
&= i \lim_{\eta \rightarrow 0} \frac{K}{2} \left(1 + \frac{F}{\pi^2\eta} \frac{q^2}{\omega^2} \right) \int (udq) \delta(u^2q^2 - \omega^2) \\
&= i \frac{K}{4} (1 + \bar{F}) \frac{1}{|\omega|}, \tag{14}
\end{aligned}$$

$$\begin{aligned}
G_R(\omega, x=0) &= i \langle \hat{\phi}_\omega^*(0) \phi_\omega(0) \rangle \\
&= i \lim_{\eta \rightarrow 0} \frac{K}{2\pi} \int udq \frac{1}{u^2q^2 - \omega^2 - i\eta\omega} = \frac{K}{4i\omega}. \tag{15}
\end{aligned}$$

Inverting the two-by-two Green's function matrix, we obtain an action that is formally equivalent to the noisy Josephson junction (2) with $R/R_Q = K$ and $C = 0$. However, we note that the fields appearing in the impurity action have a different physical meaning. In Sec. IV E, we will show how to adapt the results derived for the Josephson junction in order to obtain the current-voltage characteristics of the Luttinger liquid with a single impurity. The case of a commensurate periodic potential [i.e., $g(x) = g$ constant] is treated in Sec. V.

III. RG FRAMEWORK

In both models described above, the action of the system can be written as a sum of a quadratic and a nonquadratic term. As noted above and in Ref. 7, the quadratic part of the action is scale invariant and gives rise to a critical steady state. This provides the basis for treating the nonquadratic terms using a perturbative renormalization group (RG) method controlled by the proximity to the scale invariant steady state.

The philosophy of the RG scheme is similar to the equilibrium case. As usual, we envision measuring the system with probes of decreasing frequency resolution Λ . We should be able to compute the measured dynamic correlations using an effective Keldysh action S_Λ that has Λ as its upper cutoff in frequency instead of the larger physical cutoff Λ_0 . The effective action must be modified in such a way that all dynamical correlations at scales $\omega \leq \Lambda$ are the same as would be computed using the original action. The flow of the coefficients of the different terms in the action with the decreasing frequency scale Λ reveals the physical mechanisms that play a dominant role at each scale.

If the bare action was just the scale-invariant quadratic action, then the lower energy effective action S_Λ would of course be the same as the original action after a trivial rescaling of the coordinates and fields. By contrast, the nonlinear term g couples modes of different frequencies. Therefore the elimination of the fast modes will necessitate a change of the effective action to mimic the effect of the lost high-frequency modes on the slow modes through the mode coupling term. As long as the coupling term g is small, this change is concomitantly small and can be computed by the perturbation theory in g at each stage as we gradually eliminate shells of modes at decreasing frequency.

We now wish to make an important technical note on the implementation of the cutoff within a real-time approach. Within the imaginary time equilibrium formalism, Λ is often introduced as a sharp cutoff. This has the advantage of making a clear separation between fast and slow modes at each step of the RG. However this approach cannot be used for time-dependent problems because it violates causality.²⁹ Instead, following Refs. 31 and 30, we implement the cutoff Λ by convolving the free Green's function in the quadratic part of the action $G_0(r)$ with a smooth cutoff function $\Gamma_\Lambda = \Gamma(\Lambda r)$. As we will show, a convenient choice of the cutoff function can significantly simplify the calculations. The challenge is how to perform the integration over fast modes when there is no sharp separation between fast and slow modes in the frequency space. This is done using a technique due to Nozieres and Gallet,³⁰ which we adapt below in the nonequilibrium Keldysh framework. The derivation takes similar lines as in Refs. 8 and 9 by Mitra and one of us. Here, we generalize the scheme somewhat in order to allow application to both the one-dimensional system and to the Josephson junction. The main results of this section are summarized by Eqs. (24) and (37). These two equations give the general forms of the scaling equations to first and second orders in the strength of the cosine potential.

A. RG of a quadratic action

As a warm up, let us start by considering a quadratic action

$$S_0 = \int d^D r_1 d^D r_2 \phi(r_1) G_0^{-1}(r_1 - r_2) \phi(r_2). \tag{16}$$

Here, $r_i = (\vec{x}_i, t_i)$ is a $D = d + 1$ dimensional Keldysh coordinate, running on the forward and backward paths. For a quadratic action, the RG approach is just equivalent to rescaling the coordinates by $r_i \rightarrow (1 + dl)r_i$. The scaling equations of each parameter appearing in G_0^{-1} are determined by their respective engineering dimension. For example, unitless parameters are scale invariant and define the critical fixed points of the RG flow. Energy scales, like a finite temperature, are always relevant in an RG sense and grow along the RG flow.

At each step of the RG procedure, we need to effectively reduce the cutoff Λ by a small amount $d\Lambda = dl\Lambda$. For this purpose, we express the path-integral weight $e^{iS_0[\phi]}$ as the integral over an auxiliary field $\delta\phi$:

$$e^{i\phi G_\Lambda^{-1} \phi} = \int \mathcal{D}(\delta\phi) e^{i(\phi - \delta\phi)(G_\Lambda - dG_\Lambda)^{-1}(\phi - \delta\phi) + i\delta\phi(dG_\Lambda)^{-1}\delta\phi}. \tag{17}$$

Here, $G_\Lambda = G_0 * \Gamma_\Lambda$ and we used a shortened notation in which the integration over the coordinates is substituted by products of matrices. The function dG_Λ implements the change of the cutoff and, for an infinitesimal shift $d\Lambda$, it equals to $d\Lambda \partial_\Lambda G_\Lambda = dl\Lambda \partial_\Lambda G_\Lambda$. We now define a rescaled field $\phi' = \phi - \delta\phi$ and rewrite the RHS of Eq. (17) as $e^{iS[\phi', \delta\phi]}$, where

$$\begin{aligned}
S_0[\phi', \delta\phi] &= \int d^D r_1 d^D r_2 [\phi'(G_\Lambda - dG_\Lambda)^{-1} \phi' \\
&\quad + \delta\phi(dG_\Lambda)^{-1} \delta\phi]. \tag{18}
\end{aligned}$$

The RG procedure consists of integrating out the "fast" degrees of freedom $\delta\phi$. If the action is quadratic, the resulting

action for ϕ' is just equivalent to the original one, up to a small shift of the cutoff, $G_\Lambda - dG_\Lambda = G_{\Lambda-d\Lambda}$. If, on the other hand, the action contains nonquadratic terms, the integration out of the fast degrees of freedom can have more important effects, which are the focus of our study.

B. Perturbative RG of a nonquadratic action

Consider now an action made by the sum of two terms: a quadratic term $S_0[\phi]$ and a small nonquadratic term $S_g[\phi]$. We assume that the cutoff is implemented in the quadratic part and transform the nonquadratic part using the definition $\phi = \phi' + \delta\phi$. Next, we expand the path integral weight $e^{i(S_0+S_g)}$ in powers of S_g , integrate out the fast degrees of freedom $\delta\phi$, and re-exponentiate the resulting terms. This procedure generates a renormalized action for the “slow” fields ϕ' . Finally, we rescale the coordinates by $r \rightarrow (1 + dl)r$ to match the original cutoff and derive closed scaling equations for the parameters of S_0 and S_g .

In what follows, we will apply this scheme to a generic homogeneous nonlinear coupling of the form

$$S_g[\phi] = g \int d^D r F[\phi(r)]. \quad (19)$$

Here, $F = F(\phi)$ is some nonquadratic function of the field ϕ and $D = d + 1$ ($D = 1$ in the Josephson junction problem and $D = 2$ for the Luttinger liquid).

1. First order in g

The first-order expansion of the Keldysh weight $e^{iS} = e^{iS_0(\Lambda)+iS_g}$ gives $(1 + iS_g)e^{iS_0(\Lambda)}$. Substituting $\phi = \phi' + \delta\phi$ and integrating out $\delta\phi$, we obtain

$$1 + i\langle S_g \rangle_{\delta\phi} = 1 + ig \int d^D r \int \mathcal{D}(\delta\phi) F(\phi' + \delta\phi) e^{i(\delta\phi)(dG_\Lambda)^{-1}(\delta\phi)}. \quad (20)$$

For simplicity, we now assume $F(\phi)$ to be analytic and expand it in power series of ϕ :

$$\begin{aligned} 1 + i\langle S_g \rangle_{\delta\phi} &= 1 + ig \int d^D r \int \mathcal{D}(\delta\phi) \\ &\times \sum_n c_n (\phi' + \delta\phi)^n e^{i(\delta\phi)(dG_\Lambda)^{-1}(\delta\phi)} \\ &= 1 + iS_g[\phi'] + ig \int d^D r \sum_n \frac{n(n-1)}{2} c_n (\phi')^{n-2} \\ &\times \int \mathcal{D}(\delta\phi) (\delta\phi)^2 e^{i(\delta\phi)(dG_\Lambda)^{-1}(\delta\phi)} \\ &= 1 + iS_g[\phi'] + \frac{g}{2} dG_\Lambda(0) \int d^D r \partial_\phi^2 F(\phi'). \end{aligned} \quad (21)$$

Here, we expanded the binomial $(\phi' + \delta\phi)^n$, and we kept only the two lowest-order terms in $dG_\Lambda \sim d\Lambda$.

Finally, re-exponentiate the resulting term and rescale the coordinates by $r \rightarrow (1 + dl)r$. We obtain that the renormalized action of ϕ' differs from the original one by

$$dS^{(1)} = DdlS_g(\phi') + \frac{g}{2} dl\Lambda \frac{\partial}{\partial\Lambda} \langle \phi^2 \rangle_\Lambda \int d^D r \partial_\phi^2 F(\phi'). \quad (22)$$

The first contribution of Eq. (22) corresponds to the normal scaling of the coupling, dictated by its engineering dimensions. The second “anomalous” contribution can lead to the generation of new couplings in the action as well as to an anomalous scaling of the existing one.

As expected, if $F(\phi)$ is a quadratic function of ϕ , $\partial_\phi^2 F$ is independent of the fields and the anomalous contributions in Eq. (22) vanishes (due to cancellation of forward and backward paths). If, on the other hand, $F(\phi)$ is a periodic function of ϕ , the anomalous contribution can have the same functional dependence as the normal one. In the case of a cosine term, for instance, $F(\phi) = \cos(\phi) \Rightarrow \partial_\phi^2 F = -\cos(\phi)$ and

$$\begin{aligned} \frac{dS^{(1)}}{dl} &= DS_g[\phi'] - \Lambda \frac{1}{2} \frac{\partial}{\partial\Lambda} \langle \phi^2 \rangle_\Lambda S_g[\phi'] \\ &= \left[D - \frac{\Lambda}{2} \frac{\partial}{\partial\Lambda} G_\Lambda(0) \right] S_g[\phi']. \end{aligned} \quad (23)$$

The resulting scaling equation is

$$\frac{dg}{dl} = g \left(D - \frac{\Lambda}{2} \frac{\partial}{\partial\Lambda} \langle \phi^2 \rangle_\Lambda \right), \quad (24)$$

In general, $G_\Lambda(0) = \langle \phi^2 \rangle_\Lambda$ is an increasing function of Λ . As a consequence, the second term in the RHS of Eq. (24) tends to counterbalance the first one, eventually making it irrelevant. This is the origin of both quantum phase transitions to be described in the next two sections.

2. Second order in g

The first-order scaling equations do not include the back action of the interaction term on the quadratic terms. To account for such back action, we go on to compute the flow equations to second order in the perturbation g :

$$e^{iS_{0,\Lambda}[\phi]+iS_g[\phi]} \approx (1 + iS_g[\phi] - \frac{1}{2}S_g^2[\phi])e^{iS_{0,\Lambda}[\phi]}. \quad (25)$$

As before, we express the field ϕ as $\phi' + \delta\phi$ and average over the “fast” degrees of freedom, $\delta\phi$. Next, we re-exponentiate together the first and second orders, by using

$$1 + i\langle S_g \rangle_{\delta\phi} - \frac{1}{2}\langle S_g^2 \rangle_{\delta\phi} \approx \exp(i\langle S_g \rangle_{\delta\phi} - \frac{1}{2}S_g^2 + \frac{1}{2}\langle S_g \rangle_{\delta\phi}^2). \quad (26)$$

Here, the average denotes integration over the fast degrees of freedom $\delta\phi$, $\langle \dots \rangle = \langle \dots \rangle_{\delta\phi} = \int d(\delta\phi) \dots e^{iS_{0,\Lambda}[\phi',\delta\phi]}$. Hence the second-order correction to the effective action in terms of ϕ' is

$$dS^{(2)}[\phi'] = \frac{i}{2}\langle S_g^2 \rangle_{\delta\phi} - \frac{i}{2}\langle S_g \rangle_{\delta\phi}^2. \quad (27)$$

As usual, following the integration out of the high-frequency modes, we restore the cutoff to its original value by rescaling the coordinates $r \rightarrow (1 + dl)r$, and then rename the fields, by $\phi' \rightarrow \phi$.

In the specific case of $F[\phi] = \cos(\phi)$, we have

$$\begin{aligned} S_g[\phi] &= g \int d^D r \{\cos[\phi_+(r,t)] - \cos[\phi_-(r,t)]\} \\ &= g \sum_{\epsilon_1, \epsilon_2 = \pm} \int d^D r \epsilon_1 \epsilon_2 e^{i\epsilon_1 \phi(x,t) + i\epsilon_2 \hat{\phi}(x,t)}. \end{aligned} \quad (28)$$

Squaring this action, we obtain

$$S_g^2 = \sum_{\epsilon_i} \epsilon_1 \epsilon_2 \epsilon_3 \epsilon_4 \int d^D r_1 \int d^D r_2 e^{i\Phi_{1234}}. \quad (29)$$

Here, again r stands for the $D = d + 1$ space time coordinate and we have defined $\Phi_{1234} = \epsilon_1 \phi_1 + \epsilon_2 \hat{\phi}_1 + \epsilon_3 \phi_2 + \epsilon_4 \hat{\phi}_2$, where $\phi_i = \phi(r_i) = \phi(x_i, t_i)$.

The integration over the fast degrees of freedom and rescaling of the coordinates then gives

$$\begin{aligned} \langle S_g^2 \rangle_{d\phi} &\equiv \frac{1}{4} g^2 \sum_{\epsilon_i} \epsilon_1 \epsilon_2 \epsilon_3 \epsilon_4 (1 + dl)^{2D} \\ &\times \int d^D r_1 \int d^D r_2 e^{i\Phi_{1234}} \left(1 - dl \Lambda \frac{\partial \langle \Phi_{1234}^2 \rangle}{\partial \Lambda} \right). \end{aligned} \quad (30)$$

Using Eq. (26), we then find

$$\begin{aligned} \frac{dS^{(2)}}{dl} &= \frac{i}{8} \Lambda g^2 \prod_{i=1}^4 \sum_{\epsilon_i = \pm 1} \epsilon_1 \epsilon_2 \epsilon_3 \epsilon_4 \int dr_1 \int dr_2 e^{i\Phi_{1234}} \\ &\times \frac{\partial}{\partial \Lambda} (\langle \Phi_{1234}^2 \rangle_0 - 2\langle \phi^2 \rangle_0). \end{aligned} \quad (31)$$

$$\frac{dS^{(2)}}{dl} = \Lambda \frac{i}{4} g^2 \int dr_1 dr_2 \sum_{\epsilon_1, \epsilon_2, \epsilon_3} \epsilon_2 \epsilon_3 [\epsilon_1 (\phi_1 - \phi_2) + \epsilon_2 \hat{\phi}_1 + \epsilon_3 \hat{\phi}_2] e^{-\frac{1}{2}(\phi_1 - \phi_2)^2_0 - \frac{1}{2} \epsilon_1 \epsilon_2 \langle \hat{\phi}_1 \hat{\phi}_2 \rangle} \frac{\partial}{\partial \Lambda} (-\langle \phi_1 \phi_2 \rangle_0 + 2\epsilon_1 \epsilon_2 \langle \hat{\phi}_1 \hat{\phi}_2 \rangle_0). \quad (33)$$

We now explicitly perform the summation over ϵ_i indexes and obtain

$$\begin{aligned} \frac{dS^{(2)}}{dl} &= -\frac{1}{4} g^2 \int_{-\infty}^{\infty} d^D R \int d^D r \hat{\phi} \left(R + \frac{r}{2} \right) \hat{\phi} \left(R - \frac{r}{2} \right) \Lambda \left\{ \cos[G_{R,\Lambda}(r)] \frac{\partial G_{K,\Lambda}(r)}{\partial \Lambda} + i \sin[G_{R,\Lambda}(r)] \frac{\partial G_{R,\Lambda}(r)}{\partial \Lambda} \right\} \\ &+ \left[\phi \left(R + \frac{r}{2} \right) - \phi \left(R - \frac{r}{2} \right) \right] \hat{\phi} \left(R - \frac{r}{2} \right) \Lambda \left\{ \sin[G_{R,\Lambda}(r)] \frac{\partial G_{K,\Lambda}(r)}{\partial \Lambda} - i \cos[G_{R,\Lambda}(r)] \frac{\partial G_{R,\Lambda}(r)}{\partial \Lambda} \right\} e^{i(G_{K,\Lambda}(r) - G_{K,\Lambda}(0))}, \end{aligned} \quad (34)$$

where we defined $R = (r_1 + r_2)/2$ and $r = r_1 - r_2$. $G_{K,\Lambda} = i\langle \phi(t)\phi(0) \rangle$ and $G_{R,\Lambda} = i\langle \phi(t)\hat{\phi}(0) \rangle$ are the Keldysh and retarded components of the Green's function's in the quadratic action with a cutoff Λ .

Equation (34) amounts to a renormalization of the quadratic action (2). The first row gives the RG transformation of the Keldish component, while the second row determines the renormalization of the retarded and advanced components. These second-order contributions can be rewritten as

$$\begin{aligned} \frac{dG_K^{-1}(r)}{dl} &= \frac{i}{4} g^2 \Lambda \left(\frac{\partial}{\partial \Lambda} + \frac{\partial \langle \phi^2 \rangle}{\partial \Lambda} \right) \\ &\times \cos[G_{R,\Lambda}(r)] e^{i(G_{K,\Lambda}(r) - G_{K,\Lambda}(0))}, \end{aligned} \quad (35)$$

$$\begin{aligned} \frac{dG_R^{-1}(r)}{dl} &= \frac{i}{4} g^2 \Lambda \int dr' [(\delta(r - r') - \delta(r))] \left(\frac{\partial}{\partial \Lambda} + \frac{\partial \langle \phi^2 \rangle}{\partial \Lambda} \right) \\ &\times \sin[G_{R,\Lambda}(r')] e^{i(G_{K,\Lambda}(r) - G_{K,\Lambda}(0))}. \end{aligned} \quad (36)$$

This correction to the action includes a renormalization to the quadratic terms of the action that we can find by expanding the exponential factor in small fluctuations around its reference expectation value in the quadratic theory.^{19,30} Let us define $\delta\Phi^2 = \Phi^2 - \langle \Phi^2 \rangle_0$ and expand

$$\begin{aligned} \cos \Phi &= \sum_{n=0}^{\infty} \frac{(-1)^n}{(2n)!} (\langle \Phi^2 \rangle_0 + \delta\Phi^2)^n \\ &= \sum_{n=0}^{\infty} \frac{(-1)^n}{(2n)!} (\langle \Phi^2 \rangle_0^n + n \langle \Phi^2 \rangle_0^{n-1} \delta\Phi^2) + O(\delta\Phi^4) \\ &= e^{-\frac{1}{2} \langle \Phi^2 \rangle_0} (1 + \Phi^2 - \langle \Phi^2 \rangle_0) + O(\delta\Phi^4). \end{aligned} \quad (32)$$

The second term in the brackets renormalizes the quadratic action. The other two terms are constant contributions that can be dropped (in fact, these terms even cancel out due to the sum over the ϵ_i s). We can now substitute the definition of Φ_{1234} and plug back into Eq. (31). In doing so, we note that the contribution of terms with $\epsilon_1 = \epsilon_3$ vanishes. This is because the exponential $e^{-\frac{1}{2} \langle \Phi^2 \rangle_0}$ includes in this case the factor $\langle (\phi_1 + \phi_2)^2 \rangle_0 \rightarrow \infty$. This leads to a restricted sum only over ϵ_1, ϵ_2 , and ϵ_3 , which gives

Here, we used $G_K(0) = i\langle \phi^2 \rangle$. After a Fourier transform, they assume the more compact form

$$\begin{aligned} \frac{d}{dl} \begin{pmatrix} 0 & G_R^{-1}(\omega) \\ G_A^{-1}(\omega) & G_K^{-1}(\omega) \end{pmatrix} \\ = -\frac{\Lambda}{2} g^2 \left(\frac{\partial}{\partial \Lambda} + \frac{\partial \langle \phi^2 \rangle}{\partial \Lambda} \right) \begin{pmatrix} 0 & \mathcal{R}(\omega) - \mathcal{R}(0) \\ \mathcal{R}^*(\omega) - \mathcal{R}^*(0) & i\mathcal{K}(\omega) \end{pmatrix}. \end{aligned} \quad (37)$$

Here, ω is the Fourier conjugate to r and $\mathcal{K}(r)$ and $\mathcal{R}(r)$ are, respectively, the correlation and response function of the operator $e^{i\phi}$ in the quadratic action S_0 , already defined in Eqs. (6) and (7).

IV. THE NOISY JOSEPHSON JUNCTION

We now analyze the model of the noisy Josephson junction defined by Eq. (2). We first derive the RG equations of the Josephson junction valid up to second order in the Josephson

coupling g . We shall then analyze the flow in order to obtain a dynamical phase diagram and predict the expected current-voltage characteristics of the junction in the different regimes. We will show that there are wide regimes in which the junction exhibits manifestly nonequilibrium but nevertheless universal behavior that is controlled by the nonequilibrium critical state of the noisy RC circuit.

A. Derivation of the RG equations

Here, we give a detailed derivation of the RG equations valid to second order in the Josephson coupling constant g . Readers that are uninterested in the technical details can skip directly to the summary of the RG flow given by Eqs. (47)–(50).

Consider first the quadratic action of the RC circuit without the Josephson coupling ($g = 0$). In this case, the scaling dimension of each term of the action is just given by their engineering dimensions. The dimensionless resistance R/R_Q and the dimensionless noise strength F are scale invariant and define a *nonequilibrium* critical fixed point. However, if the resistor is kept at a nonvanishing temperature, then the temperature scales like energy and is always relevant in the RG sense, driving the system away from the above nonequilibrium critical state. The capacitance C is irrelevant in an RG sense and determines the ultraviolet cutoff of the theory: $\Lambda = 1/RC$. In what follows, we will neglect this term, and substitute it by a generic cutoff function Γ_Λ .

1. RG flow to first order in g

We now treat the effects of a weak Josephson coupling ($g \ll \Lambda$), through the perturbative RG approach presented in the previous section. The first-order scaling equation of the coupling g is given by Eq. (24) derived in Sec. III B for a generic model.

We focus at first on the zero temperature case in which the pure RC circuit would be critical. In this case, the anomalous contribution to the scaling dimension can be easily computed by inverting Eq. (3)

$$\begin{aligned} \frac{\partial}{\partial \Lambda} \langle \phi^2(t) \rangle &= 2 \frac{R}{R_Q} (1 + \bar{F}) \frac{\partial}{\partial \Lambda} \int_{-\infty}^{\infty} d\omega \frac{1}{|\omega|} \Gamma\left(\frac{|\omega|}{\Lambda}\right) \\ &= -2 \frac{R}{R_Q} (1 + \bar{F}) \frac{1}{\Lambda} \int_0^{\infty} d\omega \frac{\partial}{\partial \omega} \Gamma\left(\frac{\omega}{\Lambda}\right) \\ &= \frac{2}{\Lambda} \frac{R}{R_Q} (1 + \bar{F}). \end{aligned} \quad (38)$$

In the last identity, we used the defining properties of the cutoff function, namely that $\Gamma(x) \rightarrow 1$ for $x \rightarrow 0$ and $\Gamma(x) \rightarrow 0$ for $x \rightarrow \infty$. As expected the final result is independent on the precise form of the cutoff function. Substituting Eq. (38) into Eq. (24), we obtain the scaling equation of the Josephson coupling, valid to first order in g :

$$\frac{dg}{dl} = g \left[1 - \frac{R}{R_Q} (1 + \bar{F}) \right]. \quad (39)$$

This result agrees with the simple scaling arguments given in Ref. 7.

Let us now reintroduce the finite temperature of the bath. As we already noted, a finite temperature is a relevant

perturbation, leading at tree level to the scaling equation $dT/dl = T$. Besides this, the most important effect of a finite temperature is on the first-order renormalization of the coupling g . If we take $T > 0$, the integral in Eq. (38) is substituted by

$$K_1 = \frac{\partial}{\partial \Lambda} \int_0^{\infty} d\omega \frac{1}{\omega} [\Gamma_\Lambda(\omega) + \Gamma_\Lambda(-\omega)] \coth\left(\frac{\omega}{2T}\right). \quad (40)$$

If, for instance, we choose a cutoff of the type $\Gamma_L(\omega) = \exp(-|\omega|/\Lambda)$, we obtain

$$\begin{aligned} K_1 &= 2 \frac{1}{\Lambda^2} \int_0^{\infty} d\omega e^{-\omega/\Lambda} \coth\left(\frac{\omega}{2T}\right) \\ &= 2 \frac{T}{\Lambda} \left[\psi\left(\frac{T}{2\Lambda}\right) - \psi\left(\frac{T+\Lambda}{2\Lambda}\right) \right] - 2. \end{aligned} \quad (41)$$

Here, $\psi(x)$ is the Digamma function. For small temperatures $T \ll \Lambda$, $K_1 \approx 2$, and we retrieve the zero temperature limit (38). For high temperatures, on the other hand, the integral is proportional to $K_1 \approx \frac{T}{\Lambda}$. The precise form of the scaling function is clearly cutoff dependent, while its asymptotic behavior is general and gives $K_1 = 2(1 + \frac{T}{2\Lambda})$.

2. RG flow to second order in g

As shown in Sec. III B, the second-order contributions renormalize the quadratic part of the action, according to Eq. (37). To extract the explicit scaling equations of the different couplings, we take the low-frequency expansion of Eq. (37). The zero-frequency contribution of the Keldysh part is

$$\frac{dG_K^{-1}(\omega = 0)}{dl} = \int dt \frac{dG_K^{-1}(t)}{dl} \equiv -i \frac{g^2}{\Lambda} I_0(R/R_Q, \bar{F}). \quad (42)$$

Here, the dimensionless factor I_0 equals to

$$\begin{aligned} I_0 &= \Lambda^2 \int dt \left\{ \frac{\partial}{\partial \Lambda} + \left[\frac{\partial G_{K,\Lambda}(0)}{\partial \Lambda} \right] \right\} \mathcal{K}(t) \\ &= \Lambda^2 \int dt \left\{ \frac{t}{\Lambda} \partial_t + \left[\frac{\partial G_{K,\Lambda}(0)}{\partial \Lambda} \right] \right\} \mathcal{K}(t) \\ &= (1 - D_g) \Lambda \int dt \mathcal{K}(t), \end{aligned} \quad (43)$$

where $D_g = d \ln g / dl = 1 - R/R_Q(1 + \bar{F})$ is the scaling dimension of the junction S_g in the scale invariant steady state of the quadratic action with $1/f$ noise and the resistor at zero temperature. In writing Eq. (43), we used the fact that under these conditions, the only scale is provided by the cutoff Λ and therefore $\mathcal{K}(t)$ is a scaling function of Λt . We then integrated by parts and used Eq. (24) to obtain the result (43). In Appendix A1, we compute I_0 for a specific choice of the cutoff (A8). Here, we just note that I_0 vanishes when the noise parameter \bar{F} tends to zero and is positive for any $\bar{F} \neq 0$.

The zero-frequency component of the Keldysh action $G_K^{-1}(\omega = 0)$ can be associated with an effective temperature that is generated in the RG flow. This connection is established by comparing to the low-frequency expansion of the Keldysh component of a quadratic action at equilibrium $\eta \omega \coth(\omega/2T) = \eta T + O(\omega^2)$, where η is the dissipation (in our case, $\eta = R_Q/R$). Hence we have the mapping $G_K^{-1}(\omega = 0) \leftrightarrow \eta T$. The next term in the low-frequency

expansion of Eq. (35) is proportional to ω^2 . Comparing the coefficient of this term with the low-frequency expansion of the equilibrium form will not, in general, give the same effective temperature as inferred from the comparison of the leading term. This reflects the fact that the system is not truly at equilibrium. However, in the RG sense, the ω^2 and higher-order terms are irrelevant. Therefore the asymptotic low-frequency behavior is that of an effective equilibrium system.

Note that the corresponding correction was computed using the bare action. As the flow proceeds one should, in principle, compute this correction with the full renormalized action, and thus, in particular, with a finite temperature. This is however very complicated, in particular given the frequency dependence of the generated Keldysh term. We will thus stick to the correction computed at $T = 0$, keeping in mind that at some scale, the flow will be cut by the generated finite temperature. Note that if the system is really in equilibrium ($\bar{F} = 0$) then $I_0 = 0$ as it must be. This ensures that a zero-temperature system will not generate a finite temperature in the course of renormalization.

We turn to consider the renormalization of the off-diagonal components of the Keldysh action given by Eq. (36). The lowest-order term in the low-frequency expansion is proportional to $i\omega$:

$$\frac{dG_R^{(-1)}}{dl} = -i\omega \int dt t \frac{dG_R^{-1}(t)}{dl} \equiv -i\omega \frac{g^2}{\Lambda} I_1(\bar{F}, R/R_Q). \quad (44)$$

The coefficient I_1 is given by

$$\begin{aligned} I_1 &= \Lambda^3 \int dt t \left\{ \frac{\partial}{\partial \Lambda} + \left[\frac{\partial C_\Lambda(0)}{\partial \Lambda} \right] \right\} \mathcal{R}(t) \\ &= -D_g dl \Lambda^2 \int dt t \mathcal{K}(t). \end{aligned} \quad (45)$$

This integral is calculated explicitly in Appendix A1. By comparing Eq. (44) with the original action (2), we find that I_1 is associated with renormalization of the dissipation. Specifically, we can rewrite Eq. (44) as $d\eta/dl = I_1 g^2/\Lambda^2$, where $\eta \equiv R_Q/R$. We note that at equilibrium ($\bar{F} = 0$) I_1 vanishes, implying that then there is no renormalization of the dissipation. This is in agreement with Refs. 22,32, and 33.

The renormalization of the dissipative part in the off diagonal component of the action implies a similar renormalization of the external noise term. Recall that the $|\omega\rangle$ term in the Keldysh component was $-2i\eta|\omega\rangle - 4\pi i F|\omega\rangle$ and, as we saw above, it is not renormalized to second order in g . We can rewrite this term as $-2i(\eta + d\eta)|\omega\rangle - 4\pi i [F - d\eta/(2\pi)]|\omega\rangle$. In this way, the renormalization of the resistor in the off-diagonal term is complemented by the required renormalization in the diagonal term so as to maintain the same form as the original action (2). The price is having a renormalization of the noise term, which can be written as

$$\frac{d\bar{F}}{dl} = -\frac{g^2}{\Lambda^2} \frac{R}{R_Q} (1 + \bar{F}) I_1. \quad (46)$$

The constant I_1 is always positive, meaning that the second-order contribution acts to reduce the nonequilibrium noise. Accordingly, the renormalization of the dissipation is accom-

panied by a corresponding negative renormalization of the temperature.

3. RG equations and physical consequences

The above results can be summarized by the following scaling equations:

$$\frac{dg}{dl} = g \left[1 - \frac{R}{R_Q} \left(1 + \frac{T}{2\Lambda_0} + \bar{F} \right) \right], \quad (47)$$

$$\frac{dT}{dl} = T + \frac{R}{R_Q} \frac{g^2}{\Lambda_0} I_0 - T \frac{R}{R_Q} \frac{g^2}{\Lambda_0^2} I_1, \quad (48)$$

$$\frac{dR}{dl} = -\frac{R^2}{R_Q} \frac{g^2}{\Lambda_0^2} I_1, \quad (49)$$

$$\frac{d\bar{F}}{dl} = (\alpha - 1)\bar{F} - \frac{R}{R_Q} (1 + \bar{F}) \frac{g^2}{\Lambda_0^2} I_1. \quad (50)$$

Here, $\Lambda_0 \approx 1/(RC)$ is the bare cutoff of the junction. The unitless coefficients I_0 and I_1 are defined in Eqs. (42) and (44). As shown in Appendix A1, it is possible to obtain analytic expressions for both coefficients, by an appropriate choice of the cutoff.

Let us now review the different features of the equations (47)–(50) that describe the RG flow of the noisy shunted Josephson junction (2) up to second order in g/Λ . The flow of the Josephson coupling term given by Eq. (47) is completely analogous to the equilibrium case. The first term in the brackets reflects the engineering dimension of the Josephson coupling, which has units of energy while the remaining terms imply an anomalous scaling dimension. At equilibrium and zero temperature ($T = 0$, $\bar{F} = 0$), this equation reduces to the well known result of Refs. 34,35 with the anomalous contribution to the scaling dimension being $-R/R_Q$. Both the temperature and the noise decrease the anomalous dimension, making the Josephson coupling less relevant. At this level, the picture is identical to that given in Ref. 7, using a simple scaling argument.

New physics enters in the renormalization of the circuit at second order in g/Λ . In particular, Eq. (48) implies that a finite effective temperature of order g^2/Λ is generated in the course of renormalization even if the temperature of the resistor is zero at the outset. Physically this can be understood as follows. In absence of a mode coupling term, the energy imparted on the system by the noise is distributed exactly as dictated by the noise spectrum. For example, the spectrum of fluctuations induced by $1/f$ noise is proportional to $|\omega|$, which is very different from a thermal distribution. The effect of mode coupling is to redistribute the mode occupation and, in particular, it generates a constant contribution (i.e., frequency independent) to the distribution of fluctuations in the zero-frequency limit. The spectral weight of fluctuations at low frequencies and hence the effective temperature, can be estimated using Fermi's golden rule. First, it is proportional to g^2/Λ , which is related to the matrix elements for transitions from occupied modes at high energies to the low energies. Second, the generated effective temperature is proportional to I_0 , as defined in Eq. (42), which is related to the nonequilibrium population of high-frequency modes. As required, I_0 tends to zero at equilibrium $\bar{F} = 0$. The value of the effective

temperature is set by the ratio between the fluctuations in the zero-frequency limit and the dissipation R_Q/R .

There is also a reciprocal process due to the mode coupling term that acts to renormalize the dissipation as described by Eq. (49). It is worthwhile to write this equation directly in terms of the dissipation parameter $\eta = R_Q/R$ as

$$\frac{d\eta}{d\ell} = \frac{g^2}{\Lambda^2} I_1. \quad (51)$$

Physically, when there is a nonequilibrium population of high-frequency modes, they can absorb energy from the low-frequency modes by changing their population and thereby serve as an effective dissipative bath. The added dissipation is proportional to the coupling between the modes $(g/\Lambda)^2$ and to the coefficient I_1 , which is a measure of the deviation from equilibrium ($I_1 = 0$ for $\bar{F} = 0$). Note that, as shown in Appendix A, I_1 diverges for $(1 + \bar{F})R/R_Q < 1/2$. In this regime, the above low-frequency expansion becomes invalid. We expect that, in this regime, a nonanalytic term $\sim \omega^\mu$ with $\mu < 1$ is generated, which corresponds to sub-Ohmic dissipation. The physical implications of this transition deserve further study, which is postponed to future work.

The last equation (50) describes the scaling of the external noise. $1/f$ noise is marginal at the level of the quadratic action, but it becomes weakly irrelevant at second order in the mode coupling term. This is consistent with the system flowing toward an effective equilibrium state with a finite effective temperature.

B. RG equations at strong coupling: Duality transformation

So far we have treated the case of a weak Josephson coupling in a perturbative RG scheme to second order in the coupling g . The limit of a strong junction can be addressed by means of a well-known duality transformation,^{33,34} which is carried out in detail within the Keldysh framework in Appendix B. In the strong coupling limit, the phase across the junction is essentially locked except in rare occasions when a quantum fluctuation induces a phase slip, which can be formally described as a tunneling event of a dual particle across a weak dual junction. The current of dual particles is the rate of phase slips that gives the voltage drop on the original Josephson junction.

We can thus regard the dual junction as embedded in a complete dual circuit that is identical in structure to the original circuit with the transformations

$$\begin{aligned} g &\rightarrow g_{\text{dual}}, \\ R &\rightarrow R^{-1}, \\ F &\rightarrow (R/R_Q)^2 F, \\ T &\rightarrow T. \end{aligned} \quad (52)$$

The prefactor of the dual cosine, g_{dual} , can be evaluated using WKB approximation as³⁴ $g_{\text{dual}} \approx \Lambda \exp(-\sqrt{g/\Lambda})$. In particular, if $g \gg \Lambda$, then g_{dual} is small, facilitating the perturbative RG approach in g_{dual} . The RG equations are exactly the same as Eqs. (47)–(50) with the replacements dictated by the duality transformation (52).

C. Dynamical phase diagram

The RG flow equations derived above for the weak and strong coupling limits can serve to identify the different steady-state regimes of the system. We will show in this section that the entire parameter space is divided into three distinct regimes, which can be best described as (i) nonequilibrium superconducting, (ii) nonequilibrium insulating, and (iii) thermal metal. We shall identify the characteristic scales that define the different regimes and derive analytic expressions for the crossover lines that separate them.

We start the analysis of the dynamical regimes from the weak coupling limit, that is, when the (bare) Josephson coupling is much smaller than the cutoff $\Lambda_0 = 1/(RC)$. A rough separation into a superconducting and an insulating regimes can be made using the first-order flow of the coupling g determined by Eq. (47) with $T = 0$

$$\frac{dg}{d\ell} = g \left[1 - \frac{R}{R_Q} (1 + \bar{F}) \right]. \quad (53)$$

At this order, we would identify the insulating phase as the region $R/R_Q < (1 + \bar{F})^{-1}$, where the Josephson coupling is irrelevant and the superconducting phase as the complementary region where g flows to strong coupling.

The picture becomes somewhat more involved when we consider the second-order correction to the flow. Most importantly, Eq. (48) shows that in presence of external noise, the Josephson coupling acts to generate an effective temperature. There is always a scale Λ_T below which the temperature becomes the dominant term and where the junction will exhibit metallic behavior. But that scale may be so small that $g(\Lambda)$ meanwhile changes by orders of magnitude from its bare value. If $g(\Lambda)$ flows to strong coupling, i.e., exceeds the cutoff Λ_0 , at a scale Λ_S larger than the thermal scale Λ_T then there is a wide range of frequency scales over which the junction exhibits universal superconducting behavior. Similarly in the insulating side of Eq. (53), if $g(\Lambda)$ decreases by an order of magnitude at a scale Λ_I larger than the thermal scale then there is a wide frequency range over which the Junction exhibits insulating behavior.

Let us now estimate the scales Λ_I , Λ_S , and Λ_T . To this end, we first solve Eq. (53) to obtain $g(\ell) = g_0 \exp[(1 - \tilde{R})\ell]$, where we have defined $\tilde{R} \equiv (1 + \bar{F})R/R_Q$. When g is irrelevant ($\tilde{R} > 1$), we get the typical (logarithmic) scale $l_I = (\tilde{R} - 1)^{-1}$ and therefore $\Lambda_I = \Lambda_0 \exp[-(\tilde{R} - 1)^{-1}]$. If on the other hand, g is relevant ($\tilde{R} < 1$) it reaches the cutoff at the scale $\Lambda_S = \Lambda_0 (g_0/\Lambda_0)^{1/(1-\tilde{R})}$. Now to find the thermal scale, we substitute $g(\ell)$ into the flow equation (48) for the temperature. We then solve for $T(\ell)$ with the initial condition of zero temperature $T(0) = 0$ to obtain

$$T(\ell) = \frac{g_0^2}{\Lambda_0} \frac{I_0 R/R_Q}{2\tilde{R} - 1} [1 - e^{(1-2\tilde{R})\ell}] e^\ell \approx \frac{g_0^2}{\Lambda_0} \frac{I_0 R/R_Q}{2\tilde{R} - 1} e^\ell. \quad (54)$$

The last equality is for large l and $\tilde{R} > 1/2$, which is the regime of interest in any case. From here, we immediately obtain the thermal scale

$$\Lambda_T = I_0 \left(\frac{R/R_Q}{2\tilde{R} - 1} \right) \frac{g_0^2}{\Lambda_0} \equiv T_{\text{eff}}. \quad (55)$$

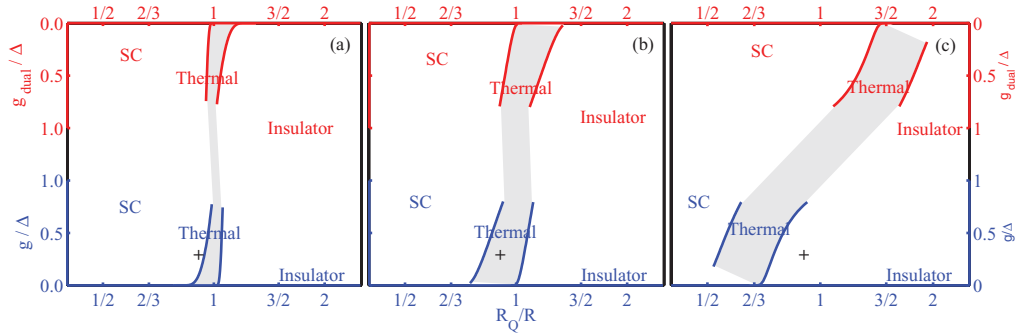


FIG. 2. (Color online) Phase diagram of the noisy Josephson junction as a function of the bare resistance R/R_Q and the bare Josephson coupling g_0/Λ_0 for different values of the noise: (a) $\bar{F} = 0.01$, (b) $\bar{F} = 0.1$, and (c) $\bar{F} = 2.0$. The blue lines (lower half of each panel) are obtained from the weak coupling analysis and correspond to Eqs. (56) and (57). The red lines (upper half of each panel) are obtained through the duality transformation. The crosses (+) indicate the points used for the numerical solution of the RG equations shown in Fig. 3.

The crossover between the superconducting and the thermal regimes in the system parameter space R/R_Q , \bar{F} , and g_0/Λ_0 is defined by the surface $\Lambda_T = \Lambda_S$, which is given by

$$\frac{g_0}{\Lambda_0} = \left[\frac{I_0 R/R_Q}{2(1 + \bar{F})R/R_Q - 1} \right]^{\frac{1-(1+\bar{F})R/R_Q}{2(1+\bar{F})R/R_Q - 1}}. \quad (56)$$

At larger values of g_0 , the junction flows to strong coupling and displays superconducting behavior over a wide frequency range.

We can find the crossover between the thermal and the insulating regimes as the surface on which the thermal scale Λ_T equals Λ_I . This crossover is given by

$$\frac{g_0^2}{\Lambda_0^2} = \frac{2(1 + \bar{F})R/R_Q - 1}{I_0 R/R_Q} e^{[1-(1+\bar{F})R/R_Q]^{-1}}. \quad (57)$$

For smaller values of g_0 , the junction displays an insulating behavior controlled by the weak coupling critical point. For larger g_0 , the effective temperature smears out the insulating behavior.

If the bare Josephson coupling is large with respect to the cutoff scale Λ_0 , one can apply the duality transformation

described above and obtain an effective description of the junction in terms of a small phase-slip fugacity. In the dual picture, the roles of the insulating and superconducting regimes are exchanged. Therefore the dual version of Eq. (56) describes the crossover between the insulating and thermal regimes, and that of Eq. (57) the crossover between the thermal and superconducting regimes.

The phase diagram derived in this way is shown in Fig. 2 for both the weak coupling and strong coupling regimes, for different values of the noise power. We see that the noise has two main effects on the phase diagram: first, it shifts the transition from superconductor to insulator away from the universal value $R_c = R_Q$. The shift is in the opposite directions for the weak and strong coupling regimes. Second, increasing noise leads to a growing crossover region that exhibits effective thermal equilibrium behavior between the two states. In the next section, we shall derive the universal transport characteristic expected in each of the three regimes.

To confirm the phase diagram obtained from the approximate solution of the RG equations, we solve Eqs. (47)–(50) numerically for various values of the bare parameters. Figure 3 shows an example of the RG flow for the following

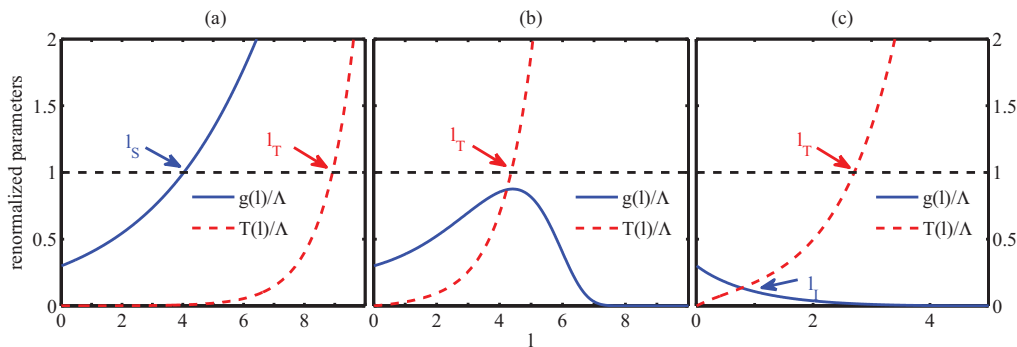


FIG. 3. (Color online) Example for RG flows of the Josephson coupling $g(l)$ and of the effective temperature $T(l)$ in the different dynamical regimes. We used the parameters $g_0/\Lambda_0 = 0.3$, $R/R_Q = 0.7$, $T_0 = 0$, and different noise parameters. (a) $\bar{F} = 0.001$, happens to be in the superconducting regime. The Josephson coupling reaches the cutoff scale Λ_0 and runs off to strong coupling before any appreciable temperature is generated. (b) $\bar{F} = 0.1$ is in the thermal metal regime. The Josephson coupling may grow initially, but the effective temperature is first to reach the cutoff scale. At lower frequency scales, the Josephson coupling is strongly suppressed by the effect of temperature. (c) $\bar{F} = 2.0$ is in the insulating regime. The Josephson coupling is irrelevant and it has a chance to decrease significantly from its bare value before the temperature reaches the cutoff scale.

set of parameters $g_0/\Lambda_0 = 0.1$, $R_0/R_Q = 0.7$, $T_0 = 0$, and $\bar{F} = 0.01, 0.1, 1.0$. These points were chosen to demonstrate a noise-driven transition and are located, respectively, in the superconducting, thermal, and insulating regimes. We see that in the superconducting regime (a) the Josephson coupling grows rapidly and reaches the cutoff scale (Λ) before the temperature does. In the thermal regime (b), the temperature grows more rapidly than the Josephson coupling, preventing the latter from reaching the cutoff scale. Finally, in the insulating regime (c), the Josephson coupling decreases significantly, before the temperature becomes dominant.

D. Current-voltage characteristics of the junction

The different dynamical regimes determined from the RG flow are characterized by distinct transport properties. Here, we derive the I - V characteristics of the junction. We find a simple universal behavior in the different regimes that nevertheless betrays the nonequilibrium nature of the system.

1. Insulating regime

The insulating state occurs in the regime where the Josephson coupling is irrelevant. We therefore expect the transport properties to be well described by a perturbative analysis in the weak coupling limit. The standard expression for the current through a voltage-biased shunted Josephson junction, to second order in the Josephson coupling g is

$$I = I_n + I_s = \frac{V}{R} + g^2 \text{Im} \mathcal{R}(\omega = eV). \quad (58)$$

Here, I_n and I_s are, respectively, the normal current and the super-current through the junction. $\mathcal{R}(\omega)$ is the response function of the operator $e^{i\theta(t)}$ in the steady state of the RC circuit unperturbed by the Josephson junction: it corresponds to the Fourier transform of Eq. (7). This perturbative calculation is sometimes referred to as the $P(E)$ approach in the context of Josephson junctions.³⁶ For voltages significantly higher than the thermal scale Λ_T , we can use the zero-temperature result (44) to obtain

$$I_s(V) = \frac{g^2}{\Lambda^2} I_1 V. \quad (59)$$

Here, $I_1 = I_1(R/R_Q, F)$ is a unitless constant whose explicit expression is given in Eq. (A9).

The above perturbative result can be improved by the RG approach. Instead of using perturbation theory on the bare model, we apply it to the renormalized model at the scale $\Lambda = V$ at which point the RG flow must be terminated. If we neglect the temperature, this gives exactly the expression (59), only with $\Lambda \rightarrow V$ and renormalized values of parameters:

$$I_s(V) = I_1(l_V) \frac{g^2(l_V)}{V}. \quad (60)$$

$$I_n(V) = \frac{V}{R(l_V)}. \quad (61)$$

Here, $I_1(l) = I_1[R(l)/R_Q, \bar{F}(l)]$ and $l_V = \log(\Lambda/V)$. We see from this that the I - V curve is a power law only at voltages

higher than the thermal scale; at smaller voltages, the Josephson coupling is suppressed by thermal fluctuations and the contribution of Cooper pair tunneling to the total current becomes negligible. In addition, the RG flow shows that the algebraic decay is actually controlled by the renormalized resistance $R[l = \log(V/\Lambda)]$ and noise $\bar{F}[l = \log(V/\Lambda)]$, rather than by their bare values. This correction is especially important if the bare Josephson coupling is large, $g_0 \gg \Lambda$, and the insulating regime is reached only as a consequence of a long RG flow. If, on the other hand, the bare Josephson coupling is small, $g_0 \ll \Lambda$, both the corrections to R and to \bar{F} are negligible and the perturbative result coincides with the RG result.

2. Superconducting regime

In the superconducting regime, the Josephson coupling runs off to strong coupling well before reaching the generated thermal scale. Therefore a perturbative analysis of the superconducting regime can be made from the dual standpoint in which the phase slip fugacity is the small parameter.

We start from a direct perturbative analysis applied to the bare dual circuit. To understand the connectivity of the dual circuit, note that a voltage bias of the original circuit corresponds to a constant current $I_{\text{dual}} = V/e$ of flux (dual particles) that flows perpendicular to the original circuit; first, across the junction and then across the resistor. The current through the original circuit corresponds, on the other hand, to the sum of the dual voltages on the junction and on the resistor. Hence, in the dual picture, we have a resistor $R_{\text{dual}} = R_Q^2/R$ connected in series with a Josephson junction $g_{\text{dual}} \ll \Lambda_0$. This is sketched in Fig. 4. (See also Appendix B for a detailed derivation of this result.)

We can now apply the weak coupling result (59) to obtain I_{dual} versus $V_{s,\text{dual}}$ on the dual Josephson element alone. Then using $I_{\text{dual}} = V$ and $V_{s,\text{dual}} = I$ and substituting the dual junction and noise parameters, we can translate the result to

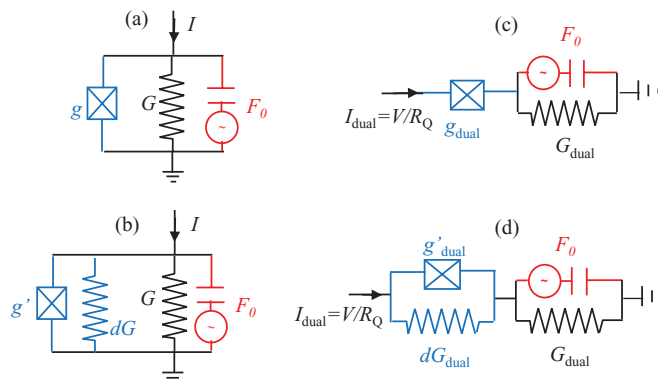


FIG. 4. (Color online) Sketch of the effective circuits used for calculating I - V characteristics. (a) Bare physical circuit. Panel (b) shows the renormalized circuit including the effective conductance δG that is generated in the course of renormalization. Panel (c) shows the bare circuit corresponding to the dual theory and (d) is the renormalized dual circuit. Note that the dual current I_{dual} can be thought of as the current of flux quanta transverse perpendicular to the junction and the resistor in panel (a).

physical voltage versus cooper pair current on the original Josephson junction:

$$V = I_1 \left(\frac{R_Q}{R}, \bar{F} \right) \frac{g_{\text{dual}}^2}{\Lambda} \left(\frac{R_Q I_s}{\Lambda} \right)^{2 \frac{R_Q}{R} (1 + \bar{F}) - 1}. \quad (62)$$

Before applying the RG approach to compute I - V relations, we should understand how the connectivity of the dual circuit changes in the course of renormalization. Under the renormalization, we generate an effective dissipation, which can be regarded as the added conductance in the circuit. The (dual) current that went through the bare Josephson junction, now splits between the junction and the conductance added in the renormalization process. This implies that the added effective dissipation is connected in parallel to the dual Josephson junction and both are connected in series to the resistor $R_{\text{dual}}(0)$ of the bare circuit as depicted in Fig. 4(b).

Now to compute the I - V relation, we take the voltage on the dual circuit as the cutoff to the RG flow $\Lambda_* = V_{\text{dual}}$. The total (dual) current is then given by

$$I_{\text{dual}} = \delta G_{\text{dual}}(l_*) V_{\text{dual}} + I_1(l_*) \frac{g_{\text{dual}}(l_*)^2}{V_{\text{dual}}}, \quad (63)$$

where $\delta G(l)$ is the renormalized conductance in parallel to the JJ at the scale l . The last relation can be immediately translated to one between the physical voltage and current:

$$V = \delta G_{\text{dual}}(l_*) I + I_1(l_*) \frac{g_{\text{dual}}(l_*)^2}{R_Q I}. \quad (64)$$

Note that δG_{dual} is proportional to $I_1 g_{\text{dual}}^2 / \Lambda$, hence both contributions to the voltage on the Josephson junction are of order g_{dual}^2 as might have been expected. The first term in Eq. (64) constitutes a small linear resistance that accompanies the emergence of effective temperature and dominates the transport at very low currents ($I/2e < T_{\text{eff}}$). In the other limit, when the current is much higher than the effective temperature, the second term in Eq. (64) dominates and leads to essentially the same result as bare perturbation theory, Eq. (62).

E. Impurity in a Luttinger liquid

As we have seen in Sec. II B, the nonequilibrium action of a local impurity in a one-dimensional system driven by $1/f$ noise can be mapped exactly to the action (2) considered here. This mapping allows us to use the results from the previous section to determine the nonequilibrium phase diagram and the current-voltage characteristics as well. In the 1D model, it is possible to induce a constant flow of particles by the transformation $\phi(x, t) \rightarrow \phi(x, t) + \pi I t$. [Recall²⁰ that the displacement field $\phi(x_0, t)$ jumps by π each time that a particles crosses the point $x = x_0$.] The flow of particles (passing through both the one-dimensional system and the impurity) is therefore equivalent to a voltage over the shunted Josephson junction (acting on both the junction and the transistor). To introduce a constant voltage in the 1D system, we need to add the following term to the Hamiltonian:

$$V \int_{-\infty}^{x_0} dx \rho(x_0) = \frac{V}{2\pi} 2\phi(x_0). \quad (65)$$

Here, $\rho(x) \approx (-1/\phi) \partial_x \phi(x)$ is the density of particles at position x . Equation (65) shows that the voltage of the 1D system (given by the sum of the voltage over the 1D lattice and the voltage over the single impurity) corresponds to the current through the noisy Josephson circuit (given by the sum of the current through the resistor and the super-current through the junction). Using this mapping, we find that current-voltage (I - V) characteristic of the noisy 1D system with a local impurity is precisely identical to the voltage-current (V - I) curve of a noisy shunted Josephson junction that we computed in Sec. IV D.

V. ONE-DIMENSIONAL SYSTEM

We turn to discuss the model of interacting particles in one dimension in a commensurate periodic potential subject to $1/f$ noise. The model was introduced in Ref. 7 and reviewed in Sec. II B. We have pointed out that, in absence of the periodic potential, the system exhibits algebraic crystalline correlations and response functions that may be very different from the equilibrium ones. The power-law decay of the correlations depends on the dimensionless ratio between the noise strength and the coupling to the bath, $\bar{F} = \pi^{-2} F / (u\eta)$. Recall that we are considering the limit where both η and F tend to zero but the ratio between them \bar{F} may be arbitrary.

Having found a scale invariant state in the quadratic model, we should ask how the nonlinear coupling of Eq. (9) behaves under the same scaling transformation. In Ref. 7, we read off the anomalous scaling dimension of the cosine term from the power-law decay exponent of the crystalline correlations (12), which gives $dg/dl = g[2 - K(1 + \bar{F})]$. This result suggests a possible noise-tuned phase transition in which the periodic potential g changes from being irrelevant to being relevant. In equilibrium ($\bar{F} = 0$), such a quantum pinning transition indeed occurs, and as can be seen from the scaling of g , it occurs at the universal value of $K = 2$.

The purpose of this article is to go beyond the simple scaling argument and account for the back action of the periodic potential on the steady-state correlations. This will be done using the general RG framework laid out in Sec. III. As mentioned above, the resulting RG equations are identical to one describing the steady state following a sudden change of the Luttinger parameter in the Sine-Gordon model. The latter problem was investigated by Mitra and one of us in Refs. 8 and 9. Without the periodic potential, the steady state following the quench exhibits algebraic correlations, as in our case, with a modified exponent that depends on the strength of the quench.³⁷ Indeed, the correlations and the response in this state are fully described by a Keldysh action almost identical to Eq. (9) except for the substitution $(\bar{F}q^2/|\omega|) \rightarrow (K_f/K_i - 1)|\omega|$, where K_i and K_f are, respectively, the Luttinger parameter before and after the quench. When building the RG equations around the Gaussian action, the different dependence on frequency and momentum ($q^2/|\omega|$ versus $|q|$) turns out to be unimportant: in the limit $\eta \rightarrow 0$, the Luttinger liquid is relativistic invariant and responds only to modes with $\omega = cq$. Since the flow will take the system away from this fixed point, some of the physics of these two problems could, however, correspond to two different fixed points.

A. RG equations

The general framework that has been laid out in Sec. III B can be directly applied to the one-dimensional system. First, we derive from the general formula (24) an explicit scaling equation for the coupling g valid to first order in the coupling. Then we use the general formula (37) for the scaling to second order in g . We carry out an expansion of this result in small frequency ω and wave vector q in order to recast the functional equation (37) as scaling equations for the set of parameters in the action (9). Readers uninterested in the technical details of the derivation can skip directly to Eqs. (71)–(76) that summarize the result.

One technical note we should make before proceeding is that for the derivation in Sec. III B, we assumed a cosine coupling of the form $\cos[\phi(x,t)]$, while we are now interested in the coupling $\cos[2\phi(x,t)]$ appearing in the action (9). We should therefore make the substitution $\phi \rightarrow 2\phi$ in the formulas appearing in Sec. III B when considering this problem.

To find the first-order flow of g explicitly, we need to compute the variation of the fluctuation $\langle\phi^2\rangle$ within the quadratic theory changing cutoff scale. Neglecting the effect of the dissipation η , we get

$$\begin{aligned} & \frac{\partial}{\partial\Lambda}\langle\phi^2\rangle \\ &= \frac{\partial}{\partial\Lambda}\lim_{\eta\rightarrow 0}\int(udq)d\omega e^{-u|q|/\Lambda}\frac{\eta\omega\cothg(\frac{\beta\omega}{2})+q^2\frac{F}{\omega}}{|\frac{1}{\pi K}(\omega^2-u^2q^2)+i\eta\omega|^2} \\ &= K\int(udq)d\omega u|q|e^{-u|q|/\Lambda} \\ & \quad \times\left[\cothg\left(\frac{\beta\omega}{2}\right)+\frac{F}{\pi^2\frac{q^2}{\omega^2}\eta}\right]\delta[\omega^2-(uq)^2] \\ &\approx K\left(1+\frac{T}{\Lambda}+\bar{F}\right). \end{aligned} \quad (66)$$

Here, we used an exponential cutoff function $\Gamma_\Lambda(q,\omega)=\exp(-u|q|/\Lambda)$ and \bar{F} is defined in Eq. (11). Substituting this result in Eq. (24) leads to the scaling equation given in Eq. (71) below.

We now turn to derive the flow equations to second order in g through an expansion of the functional equation (37) in small q and ω . A contribution with both $q=0$ and $\omega=0$ is found only in the Keldysh component $dG_K^{-1}(q,\omega)$ and is given by

$$\begin{aligned} \frac{dG_K^{-1}(\omega=0)}{dl} &= i\frac{2g^2}{\Lambda^2}\left(\Lambda\frac{\partial\langle\phi^2\rangle}{\partial\Lambda}-1\right)\int d(x/u)\int dt\mathcal{K}(x,t) \\ &= i\frac{2g^2}{\Lambda^2}(2-2D_g)\int d(x/u)\int dt\mathcal{K}(x,t) \\ &\equiv -2i\frac{g^2}{\Lambda^2}I_T(\bar{F},K). \end{aligned} \quad (67)$$

Here, D_g is the scaling dimension of the commensurate potential found from the first-order flow for vanishing temperature and dissipation, $D_g=2-K(1+\bar{F})$. $\mathcal{K}(x,t)$ is the correlation function of the operator $e^{i2\phi}$ taken in the quadratic action with $T=0$ and $\eta=0$. We used the fact that under these conditions the correlation is a scaling function of Λut and Λx , $\mathcal{K}=\mathcal{K}(\Lambda x/u,\Lambda t)$. As discussed already below Eq. (43), this

contribution to the Keldysh component can be associated with an effective temperature in the low-frequency limit through $G_K^{-1}(0,0)\leftrightarrow\eta T$. The identification is made by comparing to the low-frequency expansion of the Keldysh component at equilibrium $\eta\omega\coth(\omega/2T)=\eta T+O(\omega^2)$.

By inversion and time-reversal symmetry, $dG_K^{-1}(x,t)$ does not contain terms proportional to q or ω , and its next nonvanishing terms are proportional to q^2 and ω^2 . These terms are less relevant than the bare quadratic action, and therefore they do not affect the correlation and response functions at long times.

In contrast to the Keldysh component, the renormalization of the off-diagonal component of the action $dG_R(q,\omega)$ does not have a zero-frequency component. The lowest-order term in the gradient expansion of this term in Eq. (37) is

$$\begin{aligned} \frac{dG_R^{-1}(\omega)}{dl} &\approx i\omega\frac{g^2}{\Lambda^3}\left(2\frac{d}{dl}\langle\phi^2\rangle-3\right)\int dx\int dt\mathcal{R}(x,t) \\ &= i\frac{g^2}{\Lambda^2}(1-2D_g)\int d(x/u)\int dt\mathcal{R}(x,t) \\ &\equiv i\omega\frac{g^2}{\Lambda^3}I_\eta(\bar{F},K). \end{aligned} \quad (68)$$

This contribution amounts to renormalization of the dissipation as $d\eta/dl=i g^2/\Lambda^4 I_\eta(\bar{F},K)$.

The next order in the gradient expansion of dG_R^{-1} gives terms proportional to q^2 and ω^2 . These terms renormalize the bare term $(uK)\omega^2-(u/K)q^2$. The independent renormalization of K and u are then given by

$$\begin{aligned} \frac{dK^{-1}}{dl} &= -2dl\frac{g^2}{\Lambda^4}D_g\int d(x/u)\int dt[(x/u)^2+t^2]\mathcal{R}(x,t) \\ &\equiv dl\frac{g^2}{u^2\Lambda^4}I_K(\bar{F},K), \end{aligned} \quad (69)$$

$$\begin{aligned} \frac{du}{dl} &= -2dl\frac{g^2}{\Lambda^4}D_g\int d(x/u)\int dt[(x/u)^2-t^2]\mathcal{R}(x,t) \\ &\equiv dl\frac{g^2}{u^2\Lambda^4}I_u(\bar{F},K). \end{aligned} \quad (70)$$

The above results are summarized in the following RG scaling equations:

$$\frac{dg}{dl}=g\left[2-K\left(1+\frac{T}{\Lambda_0}+\frac{F}{\pi^2\eta}\right)\right], \quad (71)$$

$$\frac{d\eta}{dl}=\eta+\frac{g^2}{\Lambda_0^3}I_\eta, \quad (72)$$

$$\frac{d(\eta\bar{F})}{dl}=-\frac{g^2}{\Lambda_0^3}I_\eta(1+\bar{F}), \quad (73)$$

$$\frac{d(\eta T)}{dl}=2\eta T+\frac{g^2}{\Lambda_0^2}I_T, \quad (74)$$

$$\frac{dK^{-1}}{dl}=\frac{g^2}{\Lambda_0^4}I_K, \quad (75)$$

$$\frac{du}{dl}=\frac{g^2}{\Lambda_0^4}I_u. \quad (76)$$

The coefficients I_T , I_η , I_K , and I_u are defined in Eqs. (67)–(70). Analytic formulas for these coefficients as functions of

K and \bar{F} are derived in Appendix A2. It should be noted that precisely the same scaling equations were obtained in Ref. 9 in the context of a quench of a one-dimensional system in the presence of a commensurate potential. (See also Sec. II B.)

Let us briefly point to the key properties of the above scaling equations. The first-order flow of the coupling g described by Eq. (71) is very similar to the equilibrium situation but with a negative contribution of the noise through \bar{F} to the anomalous scaling dimension. It is important to note that at this order in the RG the noise, although weakening the correlation functions, is not acting as a temperature, since it preserves the power-law behavior of the correlations. One might thus expect some change in the dynamics of the particles from delocalized to localized when the noise is tuned to change g from being irrelevant to relevant. At this level, the physics is identical to that described by the simple scaling argument in Ref. 7.

As in the case of the Josephson junction, new physics is introduced by effects that are second order in the coupling g . Equation (72), for example, leads to the emergence of a finite dissipation $\eta_{\text{eff}} \sim I_\eta g^2 / \Lambda_0^3$ in the steady state although the bare dissipation $[\eta(0)]$ was infinitesimal. The analytic expression given in Eq. (A13) shows that the coefficient I_η vanishes identically at equilibrium $\bar{F} = 0$, but also that in presence of the noise, the effective dissipation diverges for $\tilde{K} \equiv K(1 + \bar{F}) < 2$ that is exactly where g becomes relevant. We can interpret this result as the emergence of sub-Ohmic dissipation that is not captured by the perturbative RG scheme. In what follows, we restrict ourselves to the regime $\tilde{K} > 2$, where η_{eff} can be made as small as we want by taking a sufficiently weak lattice. The renormalization of the dissipation generates also an effective renormalization of the noise (73), introduced to conserve constant the Keldysh part of the action.

The emergence of dissipation is accompanied by the generation of an effective temperature described by Eq. (74). We can estimate this temperature from the effective fluctuation-dissipation relation between the Keldysh and retarded parts of the action:

$$T_{\text{eff}} \approx I_T g^2 / (\eta_{\text{eff}} \Lambda^2) = \Lambda_0 I_T / I_\eta \sim \Lambda_0 (\tilde{K} - 2). \quad (77)$$

This is a rather surprising result as it implies that the temperature generated in the steady state may be large even for arbitrarily small nonlinear coupling g and noise \bar{F} . Furthermore, if we track the generated temperature as a function of the flow parameter, we see that the effective temperature reaches its large value immediately at the beginning of the flow. That is, after one infinitesimal RG iteration, we have $T(l = 0^+) = T_{\text{eff}}$. From this point of view, it looks like the nonequilibrium critical state that exists in the purely quadratic model $g = 0$, is an extremely singular limit. We shall discuss below the implications of this result and argue that the critical state of the quadratic model does nevertheless, in practice, govern the physics of the system with a weak nonlinearity.

Note that in the case of the Josephson junction discussed earlier, the effective temperature was parametrically small in both the noise strength and the nonlinear coupling. The difference between the two cases stems from the different nature of the dissipation. While the effective dissipation in the

one-dimensional system is small, of order g^2 , in the Josephson junction model, the bare dissipation is of order 1.

The scaling equations (75) and (76) for the dimensionless couplings K and u are controlled by the integrals I_K and I_u , defined in Eqs. (A14) and (A15). Though we do not have analytical expressions for these coefficients, numerical evaluation of the integrals shows that both are finite for any $\tilde{K} > 2$. Moreover, the factors I_K and I_u do not vanish in the equilibrium case $\bar{F} = 0$. This is expected given that K should also have a nontrivial flow near the Kosterlitz-Thouless transition of the Sine-Gordon model at equilibrium (see, for example, Ref. 19).

B. Nonequilibrium phase diagram

Analysis of the RG equations (71)–(76) suggests that there are at least two distinct dynamical regimes, as shown in Fig. 7. First, for $\tilde{K} = K(1 + \bar{F}) < 2$, the dissipation η diverges through the divergence of the coefficient I_η . This probably indicates generation of local sub-Ohmic dissipation, which is beyond the present RG scheme. For $\tilde{K} > 2$, an effective temperature $T_{\text{eff}} \sim (\tilde{K} - 2)\Lambda_0$ is generated immediately at the outset of the flow. We will now consider each regime separately and then move to the crossover region between them.

1. Critical thermal regime

To understand the nature of the thermal regime, recall that the source of thermalization in the system is the mode-coupling term g , which scatters the nonequilibrium population of high-frequency modes toward lower frequencies. The rate by which this scattering occurs is the generated dissipation rate $\eta_{\text{eff}} \approx I_\eta g^2 / \Lambda$. This rate sets the time scale for the system to achieve the steady state if the nonlinearity were turned on at some point in time. But, once the system reaches steady state, its effective temperature T_{eff} depends only on the energy density in the initial critical steady state and not on g . Thus the singularity of the state at $g = 0$ is resolved by the time span over which the experiment takes place. In order to see the true steady state with temperature $T \sim (\tilde{K} - 2)\Lambda_0$, we would need to conduct an experiment over a time that diverges as $\tau \sim 1/g^2$ as $g \rightarrow 0$. As a consequence, if we restrict to time scales shorter than $1/\eta_{\text{eff}}$, the system is governed by the quadratic part of the action (9) with negligible T . This is a quasisteady state, with scale invariant correlations and response given by Eqs. (12) and (13).

2. Local dissipation

As the effective Luttinger parameter decreases and approaches $\tilde{K} = 2$, the renormalization of the dissipation diverges and the dissipation constant inevitably becomes the first to reach the cutoff. The scale at which this happens is the generated effective dissipation. Clearly, at that scale, the dissipation is the largest scale in the system and we can neglect the original kinetic term $K^{-1}\omega^2$ compared to it. Therefore the effective action we should work with, below the dissipation scale $\Lambda_\eta = \eta_{\text{eff}}$ is

$$S_{\Lambda_\eta}(q, \omega) = \left(\begin{array}{cc} 0 & -\frac{u^2}{K\pi} q^2 + i\Lambda_\eta \omega \\ -\frac{u^2}{K\pi} q^2 - i\Lambda_\eta \omega & -2i\eta_0 |\omega| + F \frac{q^2}{|\omega|} + T(\Lambda_\eta) \end{array} \right) + S_g. \quad (78)$$

This describes the thermal regime of a critical theory with dynamical critical exponent $z = 2$. It is interesting to note that in this theory, the noise becomes a relevant perturbation with scaling dimension $D_F = 1$, exactly like the temperature.

3. Crossover regime

We have identified above two dynamical regimes. For $K < 2$, the renormalization of the dissipation diverges, which leads to a thermal state with short-range spatial correlations already at initial stages of the flow, that is, even at frequency scales. On the other hand, for $K \gg 2$, there is a wide range of frequency scales in which the dissipation is still small. If the finite time of the experiment does not allow for equilibration to the high effective temperature of the steady state, then the physics will be governed by the nonequilibrium critical state of the Luttinger liquid.

Of course at sufficiently small frequencies, the generated dissipation being a relevant perturbation will eventually dominate. So, the transition between the two regimes is not perfectly sharp but rather a smooth crossover. Nevertheless, we can chart the line of the crossover in the space of \tilde{K} versus the nonlinearity g by invoking similar arguments we used above for the Josephson junction. Namely, we should find the regime in \tilde{K} - g space, where a critical flow of g down by an order of magnitude can be observed before the dissipation reaches the cutoff scale where g changes by an order of magnitude.

The typical scale at which g is reduced by $1/e$ in absence of dissipation is found by solving the scaling equation for g , assuming no renormalization of the dissipation zero temperature and. The solution

$$g(l) = g_0 e^{(2-\tilde{K})l} \quad (79)$$

gives the frequency scale $\Lambda_g = \Lambda e^{(2-\tilde{K})^{-1}l}$. Now to determine the typical scale where dissipation enters significantly, we solve the scaling equation for η , see Eq. (74), while substituting the above solution for g . This gives

$$\eta(l) = I_\eta \frac{g^2}{\Lambda^3} [1 - e^{2(2-\tilde{K})l} - 1] e^l, \quad (80)$$

$$\Lambda_\eta = \frac{g_0^2}{2\Lambda^3} \frac{I_\eta}{\tilde{K} - 2}. \quad (81)$$

Here, we assumed I_η to be constant, neglecting the renormalization of the Luttinger parameter and of the sound velocity. Recalling that $I_\eta \propto (\tilde{K} - 2)^{-1}$, we find that as we move away from the transition point $\tilde{K} = 2$, the effective dissipation Λ_η decays like $(\tilde{K} - 2)^{-2}$.

Comparing Λ_η and Λ_g , we obtain an analytic expression for the crossover line between the dissipative regime and the critical regime:

$$\frac{g^2}{\Lambda^4} = \frac{2\tilde{K} - 4}{I_\eta} e^{(2-\tilde{K})^{-1}l}. \quad (82)$$

For smaller values of g , the dissipation scale is smaller than the scale for g in the critical state and it is possible to observe the critical regime. At $\tilde{K} \rightarrow 2$, the transition line goes to zero: any infinitesimal amount of nonlinearity is enough to generate an extremely strong dissipation. At large \tilde{K} , the effective

dissipation is small, but, as will see below, the effective temperature becomes large.

VI. SUMMARY AND DISCUSSION

In this paper, we investigated the physics of low-dimensional systems driven out of equilibrium by external noise sources. We considered two specific models that in equilibrium undergo interesting phase transitions: (1) a resistively shunted Josephson junction and (2) a one-dimensional quantum liquid in a commensurate lattice potential. The basic question underlying our study is whether nonequilibrium systems can exhibit universal physics. We have recently shown⁷ that such systems, in the absence of nonlinear coupling between the modes, establish a critical steady state when driven by $1/f$ noise. Here, we used this scale invariant steady state as a starting point for a controlled renormalization group analysis to treat the effect of the nonlinear couplings and thereby identify universal aspects of the nonequilibrium behavior. The perturbative RG scheme is formulated within the Keldysh path integral framework.

The scaling equation at the first order in the coupling constant indicates a transition between different regimes where the scaling dimension of a relevant operator controlling the physics of the system (Josephson coupling for the noisy Josephson junction, periodic potential of the lattice for the 1D quantum liquid) changes sign. This occurs as a direct extension of the quantum phase transitions that would exist in the corresponding system in equilibrium. Here, however, the scaling dimension can be tuned by varying the external noise strength and not only intrinsic parameters (i.e., shunt resistance or Luttinger parameter). At this level, the RG analysis is consistent with the scaling argument we gave in Ref. 7. It is important to note that at this order, although the noise is weakening the various correlation functions of the system, it is acting in a very different way than a temperature, and, in particular, preserves the power-law decay of the various correlations in the system.

The back action of the nonlinear coupling on the steady-state correlations is only given by the RG equations at the second order in the coupling. We find that generically this leads to the emergence of an effective temperature and effective dissipation in the steady state. In the case of the Josephson junction, both effects are perturbatively small, allowing the observation of a universal crossover between insulating and superconducting regimes, controlled by the above nonequilibrium quantum critical state. Using the RG approach, we obtain analytic expressions for the shape of the crossover, summarized graphically in Fig. 2. The RG approach allows us to compute the physical properties of each regime, such as the I - V characteristic of the junction shown in Figs. 5 and 6. In general, the I - V curves show an algebraic behavior, determined by the underlying critical state, followed by a thermal Ohmic behavior at voltages lower than the effective temperature.

In the one-dimensional case, we considered two types of perturbations around the critical state. The first type, a local impurity, can be mapped into the noisy shunted Josephson junction described above: the one-dimensional system plays the role of the resistor and the impurity plays the role of

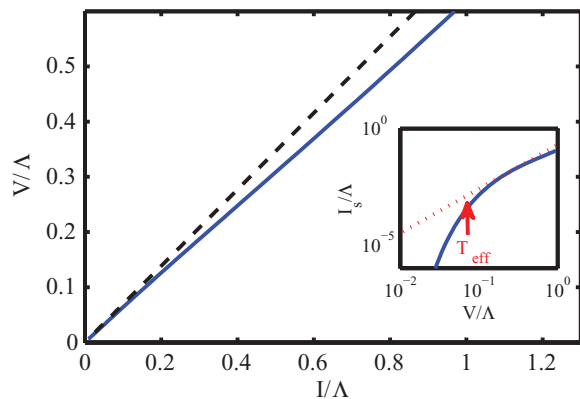


FIG. 5. (Color online) I - V characteristic of the Josephson junction in the insulating regime of the phase diagram Fig. 2, calculated from the RG flow using Eq. (61). The bare parameters of the junction are the same as the one chosen for Fig. 3(c): $g/\Lambda = 0.3$, $R/R_Q = 0.7$, and $\bar{F} = 2.0$. If the junction was a perfect insulator, all the current would flow through the resistor and the curve would be the dotted line $V = RI$. In reality, the junction carries a nonvanishing current I_s leading to a power-law deviation from the linear curve. Inset: double logarithmic plot of the supercurrent I_s . The dotted line corresponds to an ideal power law with exponent $R(l_T)/R_Q[1 + \bar{F}(l_T)]$. The actual I_s follows the power law down to the effective temperature $T_{\text{eff}} = \Lambda e^{-l_T}$.

the Josephson coupling. The second type of perturbation, a commensurate lattice, leads to new physics. Despite the different initial setup, the RG flow is equivalent to the one-dimensional quench considered in Ref. 8. The resulting nonequilibrium phase diagram shows two distinct regimes: a thermal and a dissipative regime. In the thermal regime, the lattice is irrelevant at first order. However at second order in g , the coupling of modes at all scales induced by the lattice acts to generate fluctuations and effective dissipation, both proportional to g^2 . This implies a fluctuation dissipation relation with an effective temperature of the order of the cutoff, from which the coupling g drops out. This seemingly paradoxical result is coming from an inversion of two limits, namely, the fact that the coupling to the noise can be small and the fact that one observes the steady state of the

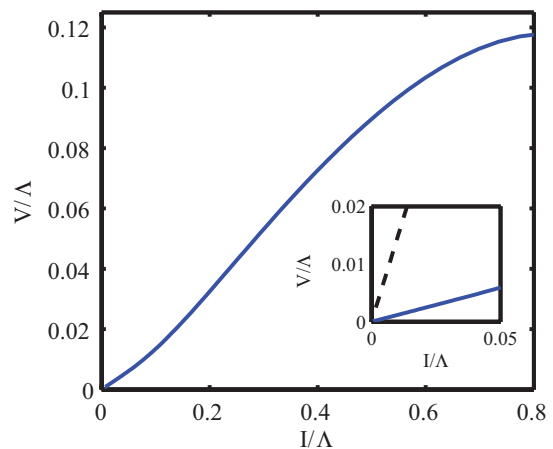


FIG. 6. (Color online) I - V characteristic of a noisy Josephson junction in the superconducting regime for $g_{\text{dual}}/\Lambda_0 = 0.3$, $R_Q/R = 0.7$, $F = 2.0$. In the regime $T_{\text{eff}} \ll I/2e \ll \Lambda_{g,\text{dual}}$, we see the algebraic behavior, predicted by the perturbation theory in the strong coupling limit, Eq. (62). In the regime $I/2e \ll T_{\text{eff}}$, highlighted in the inset, the junction follows Ohm's law with an effective resistance $\delta R = \delta G_{\text{dual}}$, perturbatively smaller than the bare resistance R (dashed line).

system at infinitely long time, allowing a large amount of energy to be pumped into the system under the form of a temperature. However, as the effective dissipation is small, the thermalization rate of the system is very small, thus allowing to observe transient nonequilibrium phenomena for relatively long times. The complete study of the dynamics of the system, in particular at transient times, goes beyond the scope of this paper and of the perturbative RG analysis, and deserves further study.

ACKNOWLEDGMENTS

We thank S. Huber, D. Huse, A. Mitra, and A. Rosch for stimulating discussions. This research was supported in part by the US-Israel binational science foundation (EA and ED), the Israel Science foundation (EA), and the Swiss NSF under MaNEP and Division II (TG). EGDT is supported by the

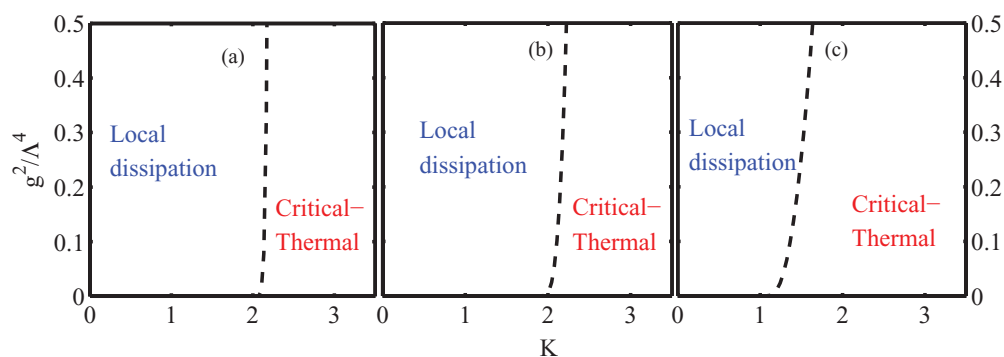


FIG. 7. (Color online) Crossover line (82) as a function of the Luttinger parameter K and the commensurate lattice strength g/Λ^2 for different values of the noise strength $\pi^{-2}F/\eta$: (a) 0.01, (b) 0.1, and (c) 1.0. In the “local dissipative” regime, the effective dissipation is diverging and the effective temperature is small, while in the “critical thermal” regime, the effective temperature is large and the dissipation small. A critical behavior is still observable in the short-times dynamics.

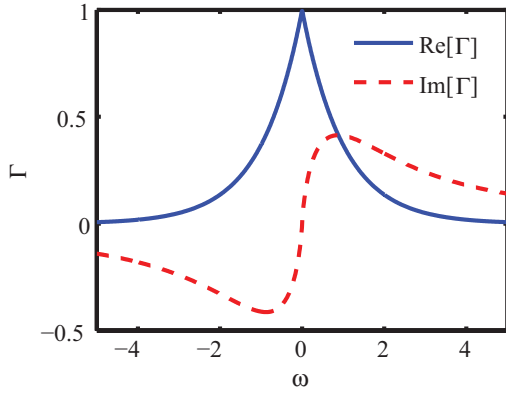


FIG. 8. (Color online) Real and imaginary parts of the cutoff function (A1). The real part of this function equals to $e^{-|\omega|/\Lambda}$. In addition, the cutoff function has a nontrivial imaginary part that allows to preserve causality.

Adams Fellowship Program of the Israel Academy of Sciences and Humanities.

APPENDIX A: EXPLICIT CALCULATION OF THE RG FLOW COEFFICIENTS

In this appendix, we show how to define a proper cutoff and use it to compute the dimensionless prefactors appearing in the scaling equations (48)–(50) and (72)–(76). Specifically, we need to obtain explicit expressions for the correlation $\mathcal{K}(x, t)$ and response $\mathcal{R}(x, t)$ of the exponential operator $e^{i\phi}$ and then use these expressions in order to compute the integrals in Eqs. (43)–(45), (68), and (70).

1. Noisy Josephson junction

The simplest choice for the cutoff would be a step function in frequency, $\Gamma(\omega/\Lambda) = 1 - \Theta(\omega/\Lambda)$. However, as we noted earlier, this choice is not valid because it violates the causality of the retarded Green's function $G_{R,\Lambda}(\omega) = G_{R,\Lambda_0}(\omega)\Gamma_\Lambda(\omega)$. Instead, we choose the following cutoff function:

$$\begin{aligned} \Gamma\left(\frac{\omega}{\Lambda}\right) &= \frac{1}{\pi} \int dv \frac{-i\omega}{(v - \omega - i0^+)(v + \omega + i0^+)} e^{-|v|/\Lambda} \\ &= e^{-|\omega|/\Lambda} + \frac{2i}{\pi} \left[-\text{CoshIntegral}\left(\frac{\omega}{\Lambda}\right) \text{Sinh}\left(\frac{\omega}{\Lambda}\right) \right. \\ &\quad \left. + \text{SinhIntegral}\left(\frac{\omega}{\Lambda}\right) \text{Cosh}\left(\frac{\omega}{\Lambda}\right) \right]. \end{aligned} \quad (\text{A1})$$

Equation (A1) explicitly preserves causality and, as shown in Fig. 8, satisfies the defining conditions of a cutoff $\Gamma_\Lambda(0) = 1$ and $\Gamma_\Lambda(\infty) = 0$.

This specific choice allows us to obtain simple expressions for the Green's functions, $G_{K,\Lambda}(t) = \langle \phi(t)\phi(0) \rangle$ and $G_{R,\Lambda}(t) = \langle \hat{\phi}(0)\phi(t) \rangle$. For convenience, we first compute the derivatives of these functions with respect to Λ . Assuming zero temperature ($T = 0$), we obtain

$$\begin{aligned} \frac{\partial G_{K,\Lambda}(t)}{\partial \Lambda} &= i \frac{R}{R_Q} (1 + \bar{F}) \frac{\partial}{\partial \Lambda} \int d\omega e^{i\omega t} \frac{1}{\omega} \left[\Gamma\left(\frac{\omega}{\Lambda}\right) + \Gamma\left(-\frac{\omega}{\Lambda}\right) \right] \\ &= i \frac{R}{R_Q} (1 + \bar{F}) \frac{1}{\Lambda^2} \int_{-\infty}^{\infty} dv e^{-|v|/\Lambda} (e^{i\omega t} + e^{-i\omega t}) \\ &= 2i \frac{R}{R_Q} (1 + \bar{F}) \frac{-2/\Lambda}{1 + \Lambda^2 t^2}, \end{aligned} \quad (\text{A2})$$

$$\begin{aligned} \frac{\partial G_{R,\Lambda}(t)}{\partial \Lambda} &= \frac{R}{R_Q} \frac{\partial}{\partial \Lambda} \int d\omega e^{i\omega t} \Gamma\left(\frac{\omega}{\Lambda}\right) \frac{1}{i\omega t} \\ &= \frac{R}{R_Q} \frac{1}{\Lambda^2} \int_{-\infty}^{\infty} (udq) e^{-u|q|/\Lambda} (e^{iqt} - e^{-iqt}) \\ &= 2 \frac{R}{R_Q} \Theta(t) (1 + \bar{F}) \frac{-2t}{1 + \Lambda^2 t^2}. \end{aligned} \quad (\text{A3})$$

Here, $\Theta(t)$ is the Heaviside step function. We can now integrate with respect to Λ and obtain

$$G_{K,\Lambda}(t) = G_{K,\Lambda}(0) + 2i \frac{R}{R_Q} (1 + \bar{F}) \ln(1 + \Lambda^2 t^2), \quad (\text{A4})$$

$$G_{R,\Lambda}(t) = 2\Theta(t) \frac{R}{R_Q} \arctan\left(\frac{t}{\Lambda}\right). \quad (\text{A5})$$

The correlation and response functions of the exponential operator $e^{i\theta}$ are, in turn, simple functions of the Green's functions $G_{K,\Lambda}$ and $G_{R,L}$:

$$\begin{aligned} \mathcal{K}(t) &= \langle e^{i\theta(t)+i\hat{\theta}(t)} [e^{-i\theta(0)-i\hat{\theta}(0)} + e^{i\theta(0)-i\hat{\theta}(0)}] \rangle \\ &= e^{-\frac{1}{2}(\langle \theta(t)+\hat{\theta}(t)-\theta(0)-\hat{\theta}(0) \rangle^2)} + e^{-\frac{1}{2}(\langle \theta(t)+\hat{\theta}(t)-\theta(0)-\hat{\theta}(0) \rangle^2)} \\ &= 2 \cos[G_{R,\Lambda}(t')] e^{i[G_{K,\Lambda}(t) - G_{K,\Lambda}(0)]}, \end{aligned} \quad (\text{A6})$$

$$\begin{aligned} \mathcal{R}(t) &= \langle e^{i\theta(t)+i\hat{\theta}(t)} [e^{-i\theta(0)-i\hat{\theta}(0)} - e^{i\theta(0)-i\hat{\theta}(0)}] \rangle \\ &= 2 \sin[G_{R,\Lambda}(t')] e^{i[G_{K,\Lambda}(t) - G_{K,\Lambda}(0)]}. \end{aligned} \quad (\text{A7})$$

Here, we used $G_K = i\langle \theta\theta \rangle$, $G_R = i\langle \hat{\theta}\hat{\theta} \rangle$, and $\langle \hat{\theta}\hat{\theta} \rangle = 0$.

We now use these expressions together with the first-order result (38) to derive the I_0 and I_1 , defined in Eqs. (43) and (45),

$$\begin{aligned} I_0 &= \left[2 \frac{R}{R_Q} (1 + \bar{F}) - 1 \right] \int_{-\infty}^{\infty} dt \cos \left[2 \frac{R}{R_Q} \text{artg}(\Lambda t) \right] \left(\frac{1}{1 + \Lambda^2 t^2} \right)^{\frac{R}{R_Q} (1 + \bar{F})} \\ &= \left[2 \frac{R}{R_Q} (1 + \bar{F}) - 1 \right] \int_{-\pi/2}^{\pi/2} dy \cos \left(2 \frac{R}{R_Q} y \right) (\cos y)^{2 \frac{R}{R_Q} (1 + \bar{F}) - 2} = \frac{4\pi}{2^{2R/R_Q(1+\bar{F})}} \frac{1}{B\left[\frac{R}{R_Q} \bar{F}, \frac{R}{R_Q} (2 + \bar{F})\right]}, \quad (\text{A8}) \\ I_1 &= \left[2 \frac{R}{R_Q} (1 + \bar{F}) - 2 \right] \int_{-\infty}^{\infty} dt t \sin \left[2 \frac{R}{R_Q} \text{artg}(\Lambda t) \right] \left(\frac{1}{1 + \Lambda^2 t^2} \right)^{\frac{R}{R_Q} (1 + \bar{F})} \\ &= 2 \left[2 \frac{R}{R_Q} (1 + \bar{F}) - 2 \right] \int_0^{\pi/2} dy \sin \left(2 \frac{R}{R_Q} y \right) (\cos y)^{2 \frac{R}{R_Q} (1 + \bar{F}) - 2} \tan(y) \end{aligned}$$

$$\begin{aligned}
&= 4 \frac{R}{R_Q} \int_0^{\pi/2} dy \cos\left(2 \frac{R}{R_Q} y\right) (\cos y)^{2 \frac{R}{R_Q} (1+\bar{F})-2} \\
&= \frac{4\pi R/R_Q}{2^{2R/R_Q(1+\bar{F})} \left[2 \frac{R}{R_Q} (1+\bar{F}) - 1\right] B\left[\frac{R}{R_Q} \bar{F}, \frac{R}{R_Q} (2+\bar{F})\right]}.
\end{aligned} \tag{A9}$$

Here, $B(x, y) = \Gamma(x+y)/\Gamma(x)\Gamma(y)$ is the Bigamma function. This function diverges if $x = 0$ and $y \neq 0$, implying that both I_0 and I_1 vanish at equilibrium ($\bar{F} = 0$). In addition, we note that Eq. (A9) is valid only for $2 \frac{R}{R_Q} (1+\bar{F}) > 1$, while for $2 \frac{R}{R_Q} (1+\bar{F}) < 1$ the integral diverges.

2. One-dimensional system

We now move to the one-dimensional system. Here, the natural choice of the cutoff is $\Gamma(q, \omega) = e^{-u|q|/\Lambda}$. The correlation and response function of ϕ are then given by

$$\begin{aligned}
G_K(x, t) - G_K(0, 0) &= i \frac{1}{2} \langle [\phi(x, t) - \phi(0, 0)]^2 \rangle \\
&= i \frac{K}{4} \int (udq) d\omega (1 - e^{iq\delta x - i\omega\delta t}) e^{-u|q|/\Lambda} \\
&\quad \times \left(1 + \frac{F}{\pi^2 \eta} \frac{q^2}{\omega^2}\right) \delta(\omega^2 - u^2 q^2) \\
&= i \frac{K}{4} (1 + \bar{F}) \{ \ln[|1 + \Lambda(x/u - t)|] \\
&\quad + \ln[|1 + \Lambda(x/u + t)|] \}, \tag{A10}
\end{aligned}$$

$$\begin{aligned}
G_R(x, t) &= i \langle \hat{\phi}(x, t) \phi(0, 0) \rangle \\
&= \lim_{\eta \rightarrow 0} \int (udq) d\omega e^{iqx - i\omega t} e^{-u|q|/\Lambda} \frac{1}{\omega^2 - u^2 q^2 - i\eta\omega} \\
&= \frac{K}{2} \Theta(t) \{ \text{artg}[\Lambda(x/u + t)] + \text{artg}[\Lambda(x/u - t)] \}. \tag{A11}
\end{aligned}$$

Here, we have neglected the effects of both the dissipation and the temperature ($\eta = T = 0^+$) and \bar{F} is defined in Eq. (11).

Substituting these expressions in Eqs. (67)–(70), we find

$$\begin{aligned}
I_T &= (2\tilde{K} - 2) \int_{-\infty}^{\infty} dx \int_{-\infty}^{\infty} dt \cos[K \text{artan}(x+t) \\
&\quad - K \text{artan}(x-t)] \left[\frac{1}{1+(x+t)^2} \right]^{\tilde{K}/2} \left[\frac{1}{1+(x-t)^2} \right]^{\tilde{K}/2} \\
&= 4(\tilde{K} - 1) \int_0^{\infty} du \cos[K \text{artan}(u)] \left(\frac{1}{1+u^2} \right)^{\tilde{K}/2} \\
&\quad \times \int_0^{\infty} dv \cos[(K \text{artan}(v))] \left(\frac{1}{1+v^2} \right)^{\tilde{K}/2} \\
&= (\tilde{K} - 1) \left[\frac{4\pi}{2^{\tilde{K}}} \frac{1}{(\tilde{K} - 1) B\left(\frac{\tilde{K}+K}{2}, \frac{\tilde{K}-K}{2}\right)} \right]^2, \tag{A12}
\end{aligned}$$

$$\begin{aligned}
I_\eta &= (2\tilde{K} - 3) \int_{-\infty}^{\infty} dx \int_0^{\infty} dt t \sin[K \text{artan}(x+t) \\
&\quad - K \text{artan}(x-t)] \left[\frac{1}{1+(x+t)^2} \right]^{\tilde{K}/2} \left[\frac{1}{1+(x-t)^2} \right]^{\tilde{K}/2}
\end{aligned}$$

$$\begin{aligned}
&= 4 \left(\tilde{K} - \frac{3}{2} \right) \int_0^{\infty} du \cos[K \text{artan}(u)] \left(\frac{1}{1+u^2} \right)^{\tilde{K}/2} \\
&\quad \times \int_0^{\infty} dv v \sin[K \text{artan}(v)] \left(\frac{1}{1+v^2} \right)^{\tilde{K}/2} \\
&= 4 \left(\tilde{K} - \frac{3}{2} \right) \cos[K \text{artan}(u)] \left(\frac{1}{1+u^2} \right)^{\tilde{K}/2} \int_0^{\infty} \frac{K}{\tilde{K}/2-1} \\
&\quad \times \int_0^{\infty} dv \cos[K \text{artan}(v)] \left(\frac{1}{1+v^2} \right)^{\tilde{K}/2} \\
&= \frac{(\tilde{K} - \frac{3}{2})}{2(\tilde{K} - 1)(\tilde{K} - 2)} I_T, \tag{A13}
\end{aligned}$$

$$\begin{aligned}
I_K &= (2\tilde{K} - 4) \int_{-\infty}^{\infty} dx \int_0^{\infty} dt \{x^2 + t^2 \sin[K \arctan(x+t) \\
&\quad - K \arctan(x-t)]\} \left[\frac{1}{1+(x+t)^2} \frac{1}{1+(x-t)^2} \right]^{\frac{\tilde{K}}{2}}, \tag{A14}
\end{aligned}$$

$$\begin{aligned}
I_u &= (2\tilde{K} - 4) \int_{-\infty}^{\infty} dx \int_0^{\infty} dt \{x^2 - t^2 \sin[K \arctan(x+t) \\
&\quad - K \arctan(x-t)]\} \left[\frac{1}{1+(x+t)^2} \right]^{\tilde{K}/2} \left[\frac{1}{1+(x-t)^2} \right]^{\tilde{K}/2}. \tag{A15}
\end{aligned}$$

In the absence of the noise ($F/\eta = 0 \Rightarrow \tilde{K} = K$), both I_T and I_η go to zero. As expected at equilibrium, the nonlinear coupling does not lead to a renormalization of the temperature or of the dissipation. Also note that, for any finite noise strength, I_η diverges at $\tilde{K} = 2$, while I_T remains finite at this point. This observation will have dramatical consequences on the properties of the expected nonequilibrium phase transition,⁷ located precisely at $\tilde{K} = 2$.

For the integrals I_K and I_u , we were not able to find an analytic solution. However, we have numerically computed them and found that, in agreement with the known equilibrium results,¹⁹ both integrals do not vanish even in the absence of the noise. In addition, we found that both I_K and I_u are finite for any $\tilde{K} > 2$. For details about their behavior around the $\tilde{K} = 2$ point, the reader is referred to Ref. 9.

APPENDIX B: DUALITY TRANSFORMATION

In this Appendix, we review how the duality transformation^{33,34,38} works within the real-time Keldysh framework. Our starting point is the nonequilibrium Keldysh action (2), which we split into a unitary part and a dissipative or nonlocal part $S = S_u + S_{\text{dis}}$. The unitary part of the action

includes the capacitor C and the Josephson coupling g , while the nonlocal terms include the resistor and the external noise.

In the strong coupling limit ($g \gg \Lambda$), the unitary action is large justifying the use of a saddle point approximation for the phase dynamics of the field θ . This leads to two independent equations of motion for the fields $\phi_{\pm}(t)$ on the forward and backward branches of the Keldysh contour:

$$\frac{\delta S_{\text{Re}}}{\delta \phi_{\pm}} = (RC)\partial_t^2 \phi_{\pm}(t) - g \sin[\phi_{\pm}(t)] = 0. \quad (\text{B1})$$

Equation (B1) has instanton solutions $\phi(t) = 2\pi\epsilon_s f(t - t_0)$, where $\epsilon_s = \pm 1$ and $f(t)$ is a step function broadened by a short time scale $\tau = \sqrt{C/g}$. The instanton solution describes a jump of the phase (phase slip) by $\pm 2\pi$ between minima of the cosine potential. A more general saddle point solution can include any number n_+ of instantons in the forward and n_- instantons in the backward branches of the Keldysh contour. Furthermore, in the strong coupling limit phase slips are rare, in the sense that the average time between them is much larger than the instanton time τ . In this case, we can take a general saddle point solution to be a sum of independent instantons and at the same time regard each instanton as a step function,

$$\phi_{\pm}(t) = \sum_{i=1}^{n_{\pm}} \epsilon_{\pm,i} \Theta(t - t_{\pm,i}). \quad (\text{B2})$$

Here, $t_{\pm,i}$ is the time of the instanton. Plugging these solutions into the Keldysh action, the path integral is converted to a sum over all possible instanton configurations on the two branches:

$$\int \mathcal{D}\phi_+ \mathcal{D}\phi_- e^{iS[\phi_+, \phi_-]} = \sum_{\alpha=\pm} \sum_{c_{\alpha}} \frac{1}{n_{\alpha}!} \exp(i\alpha n_{\alpha} S_{\text{ins}} + iS_{\text{dis}}[c_+, c_-]). \quad (\text{B3})$$

Here, $c_{\pm} = \{n_{\pm}, \epsilon_{\pm,i}, t_{\pm,i}\}$ denotes an instanton configuration on the forward/backward branch and S_{ins} is the action of a single instanton.

The nonlocal part of the action $S_{\text{dis}}[c_+, c_-]$ can be written explicitly in terms of the instanton coordinates $t_{i,\alpha}$ and $\epsilon_{i,\alpha} = \pm$ by plugging the instanton solutions into the the quadratic form of the original action action,

$$\begin{aligned} S_{\text{dis}} &= \sum_{\alpha, \beta=\pm} \int dt \int dt' \phi_{\alpha}(t) (G_{\text{dis}}^{-1})_{\alpha\beta}(t - t') \phi_{\beta}(t') \\ &= \sum_{\alpha, \beta} \sum_{i, j=1}^{n_{\pm}} \epsilon_{\alpha,i} \epsilon_{\beta,j} \int_{-\infty}^{t_{\alpha,i}} dt_1 \int_{-\infty}^{t_{\beta,j}} dt_2 (G_{\text{Im}}^{-1})_{\alpha\beta}(t_1 - t_2). \end{aligned} \quad (\text{B4})$$

This part of the action contributes a pairwise interaction between instantons at different times.

We now introduce the dual field $\theta_{\alpha}(t)$ through the identity

$$\begin{aligned} e^{iS_{\text{dis}}[\epsilon_i, t_i]} &= \int \mathcal{D}\theta \exp \left[i \sum_{\alpha, \beta} \alpha \beta \int d\omega \omega^2 \theta^{\alpha}(-\omega) G_{\text{dis}}(\omega)_{\alpha\beta} \theta^{\beta}(\omega) \right. \\ &\quad \left. + \sum_{\alpha} \sum_{i=1}^{n_{\alpha}} \alpha \epsilon_{\alpha,i} \theta_{\alpha}(t_i) \right]. \end{aligned} \quad (\text{B5})$$

Substituting this back into Eq. (B3), we can perform the summation over n_{α} as follows:

$$\begin{aligned} &\sum_{n_{\alpha}} \frac{1}{n_{\alpha}!} \exp \left[i n_{\alpha} S_{\text{sol}} + i \sum_{i=1}^{n_{\alpha}} \epsilon_{\alpha,i} \theta_{\alpha}(t_i) \right] \\ &= \sum_n \frac{1}{(n)!} \left[\sum_{\epsilon, t} e^{iS_{\text{sol}} + i\epsilon \theta_{\alpha}(t)} \right]^n \\ &= \exp \left\{ \sum_t e^{iS_{\text{sol}}} \cos[\theta_{\alpha}(t)] \right\} \\ &\equiv \exp \left(i g_{\text{dual}} \int dt \{\cos[\theta_{\alpha}(t)]\} \right). \end{aligned} \quad (\text{B6})$$

Here, we used the time scale RC to transform the sum over times into an integral. The phase slip fugacity $g_{\text{dual}} = (1/RC)e^{iS_{\text{sol}}}$ can be estimated using the WKB approximation³⁴ to be $g_{\text{dual}} \approx (1/RC)e^{-\sqrt{gRC}}$.

Finally, putting Eq. (B6) together with Eq. (B5), we obtain the dual action

$$\begin{aligned} S &= \sum_{\alpha, \beta} \int d\omega \theta_{\alpha}(-\omega) (G_{\text{dual}}^{-1})^{\alpha\beta} \theta_{\beta}(\omega) \\ &\quad + g_{\text{dual}} \int dt \cos(\theta_+) - \cos(\theta_-). \end{aligned} \quad (\text{B7})$$

Here we defined $G_{\text{dual}}^{-1}(\omega)_{\alpha\beta} = \alpha\beta\omega^2 G_{\text{dis}}(\omega)_{\alpha\beta}$.

To compare the dual model (B7) with the original one (2), it is useful to express G_{dual}^{-1} in terms of its classical and quantum components:

$$\begin{pmatrix} 0 & G_{\text{dual}}^{-1,R} \\ G_{\text{dual}}^{-1,A} & G_{\text{dual}}^{-1,K} \end{pmatrix} = \omega^2 \begin{pmatrix} 0 & G_{\text{Im}}^A \\ G_{\text{Im}}^R & -G_{\text{Im}}^K \end{pmatrix}. \quad (\text{B8})$$

Using Eq. (2), we obtain

$$G_{\text{dual}}^{-1} = \begin{pmatrix} 0 & i \frac{R}{R_Q} \omega \\ -i \frac{R}{R_Q} \omega & -2i \frac{R^2}{R_Q^2} \left[\frac{R_Q}{R} \omega \coth(\omega/2T) + F \omega^{2-\alpha} \right] \end{pmatrix}. \quad (\text{B9})$$

By inspection we see that the dual action is identical to the original one, up to the duality transformation $R/R_Q \rightarrow R_Q/R$, $F \rightarrow (R/R_Q)^2 F$, $T \rightarrow T$, and $g \rightarrow g_{\text{dual}}$. In this sense, the shunted Josephson junction is self dual even in the presence of the external noise.

In the above derivation, we implicitly assumed that the junction is disconnected from external sources apart from the noise source. However, to derive the current-voltage characteristics, we need to embed the junction in a circuit with applied current or voltage bias and to generalize the duality transformation to this case. The question is how the circuit structure transforms under the duality transformation.

Consider the circuit shown in Fig. 4(a) in which the noise-driven shunted Josephson junction is biased by a DC current. The current can be enforced by adding the term $S_I = I \int dt \phi(t)$ to the Keldysh action (2), which transforms the periodic cosine potential into a wash-board potential. If the current is small compared to g , we can still substitute the soliton solutions obtained above into the action. Doing this for the new term S_I we obtain $S_I = 2\pi I \sum_{\alpha=\pm} \sum_i \alpha \epsilon_{i,\alpha} t_{i,\alpha}$. Introducing the dual field θ as before and summing over n , we

get

$$S = \sum_{\alpha,\beta} \int d\omega \omega^2 \theta_{\alpha}(-\omega) (G_{\text{dual}}^{-1})_{\alpha,\beta} \theta_{\beta}(\omega) + g \int dt \cos[\theta_{+}(t) + 2\pi I t] - \cos[\theta_{-}(t) + 2\pi I t] \quad (\text{B10})$$

[here, we work in the units for which $\hbar = 1$ and $R_Q = h/(2e)^2 = 2\pi$]. Equation (B10) shows that a current I acts in the dual circuit as a voltage bias $V_{\text{dual}} = R_Q I$, applied only to the Josephson junction (and not to the resistor). In this sense, the dual model corresponds to a circuit in which the Josephson junction is connected in series to the resistor [see Fig. 4(c)].

We will now show that the duality transformation maps the voltage across the original circuit into the current of the dual circuit. The voltage can be obtained formally by taking the derivative of the Keldysh path integral with respect to separate current sources I_{+} and I_{-} acting in the forward and backward directions and setting $I_{+} = I_{-} = I$ in the end:

$$\langle V(t) \rangle = \partial_t \langle \theta(t) \rangle = \partial_t \int d\theta \left[\frac{d}{dI_{+}(t)} - \frac{d}{dI_{-}(t)} \right] e^{iS[I_{+}, I_{-}]} \Big|_{I_{\pm}=I} \equiv 2\pi g_{\text{dual}} \partial_t \int t d\theta [\sin(\theta_{+} + 2\pi I t) + \sin(\theta_{-} + 2\pi I t)] t e^{iS_{\text{dual}}}. \quad (\text{B11})$$

As the junction is in a steady state, $\langle V(t) \rangle$ is independent on t and we can take, for example, $t = 0$:

$$\langle V \rangle = 2\pi g_{\text{dual}} \int d\theta [\sin(\theta_{+}) + \sin(\theta_{-})] e^{iS_{\text{dual}}} \equiv 2\pi \langle I_{\text{dual}}^S \rangle. \quad (\text{B12})$$

We see from the last expression that $\langle V(t) \rangle = R_Q I_{\text{dual}}^S$ by definition of the supercurrent through the dual junction.

Equations (B10) and (B12) can be used to evaluate the I - V characteristic of the original circuit in the strong coupling regime. (The calculation follows the same steps used to compute the current across the junction in the weak coupling regime.) In the strong coupling regime, $g \gg \Lambda \Rightarrow g_{\text{dual}} \ll \Lambda$ and we can apply first-order perturbation theory in g_{dual} to find

$$\langle V \rangle = i g_{\text{dual}}^2 \int_{-\infty}^0 dt' \{ \cos[\theta_{+}(t') + 2\pi I t'] - \cos[\theta_{-}(t') + 2\pi I t'] \} \{ \sin(\theta_{+}(0)) + \sin(\theta_{-}(0)) \} \rangle_0. \quad (\text{B13})$$

Here, $\langle \dots \rangle_0$ is the average with respect to the quadratic part of the Keldysh action (B7). Finally, we exploit causality to extend the integral from $t' = 0$ to $t' = \infty$ and rewrite Eq. (B13) as

$$\langle V \rangle = g_{\text{dual}}^2 \text{Im} \left\{ \int_{-\infty}^{\infty} dt' e^{i2\pi I t'} \langle [e^{i\theta_{+}(t')} - e^{i\theta_{-}(t')}] \times [e^{i\theta_{+}(0)} + e^{i\theta_{-}(0)}] \rangle_0 \right\} \equiv g_{\text{dual}}^2 \text{Im}[\mathcal{R}(\omega = 2\pi I)]. \quad (\text{B14})$$

Here, $\mathcal{R}(\omega)$ is the Fourier transform of the response function of the operator $e^{i\theta}$.

¹A. A. Clerk, S. M. Girvin, F. Marquardt, and R. J. Schoelkopf, *Rev. Mod. Phys.* **82**, 1155 (2010).

²J. Clarke and F. K. Wilhelm, *Nature (London)* **453**, 1031 (2008).

³R. J. Schoelkopf and S. M. Girvin, *Nature (London)* **451**, 664 (2008).

⁴I. Bloch, J. Dalibard, and W. Zwerger, *Rev. Mod. Phys.* **80**, 885 (2008).

⁵A. Polkovnikov, K. Sengupta, A. Silva, and M. Vengalattore, *Rev. Mod. Phys.* **83**, 863 (2011).

⁶A. Tomadin, S. Diehl, and P. Zoller, *Phys. Rev. A* **83**, 013611 (2011).

⁷E. D. Torre, E. Demler, T. Giamarchi, and E. Altman, *Nat. Phys.* **6**, 806 (2010).

⁸A. Mitra and T. Giamarchi, *Phys. Rev. Lett.* **107**, 150602 (2011).

⁹A. Mitra and T. Giamarchi, *Phys. Rev. B* **85**, 075117 (2012).

¹⁰J. Bonart, L. F. Cugliandolo, and A. Gambassi, e-print arXiv:1109.4107.

¹¹G. Zimmerli, T. M. Eiles, R. L. Kautz, and J. M. Martinis, *Appl. Phys. Lett.* **61**, 237 (1992).

¹²G. Ithier, E. Collin, P. Joyez, P. J. Meeson, D. Vion, D. Esteve, F. Chiarello, A. Shnirman, Y. Makhlin, and J. Schrieffer, *Phys. Rev. B* **72**, 134519 (2005).

¹³J. M. Martinis, S. Nam, J. Aumentado, K. M. Lang, and C. Urbina, *Phys. Rev. B* **67**, 094510 (2003).

¹⁴R. Barends *et al.*, *Appl. Phys. Lett.* **99**, 113507 (2011).

¹⁵R. P. Feynman and F. L. Vernon, *Ann. Phys.* **24**, 118 (1963).

¹⁶A. O. Cladeira and A. J. Leggett, *Physica A* **121**, 587 (1983).

¹⁷A. Kamenev and A. Levchenko, *Adv. Phys.* **58**, 197 (2009).

¹⁸F. D. M. Haldane, *Phys. Rev. Lett.* **47**, 1840 (1981).

¹⁹T. Giamarchi, *Quantum Physics in One Dimension* (Oxford University Press, Oxford, 2004).

²⁰T. Giamarchi, in *Lectures on the Physics of Highly Correlated Electron Systems X*, edited by A. Avella and F. Mancini, AIP Conference Series, Vol. 846 (American Institute of Physics, Melville, NY, 2006), pp. 94–129.

²¹M. A. Cazalilla, R. Citro, T. Giamarchi, E. Orignac, and M. Rigol, *Rev. Mod. Phys.* **83**, 1405 (2011).

²²C. L. Kane and M. P. A. Fisher, *Phys. Rev. B* **46**, 15233 (1992).

²³D. Jaksch, C. Bruder, J. I. Cirac, C. W. Gardiner, and P. Zoller, *Phys. Rev. Lett.* **81**, 3108 (1998).

²⁴M. Carrega, D. Ferraro, A. Braggio, N. Magnoli, and M. Sassetti, *Phys. Rev. Lett.* **107**, 146404 (2011).

²⁵L. Deslauriers, S. Olmschenk, D. Stick, W. K. Hensinger, J. Sterk, and C. Monroe, *Phys. Rev. Lett.* **97**, 103007 (2006).

²⁶J. Labaziewicz, Y. Ge, D. R. Leibbrandt, S. X. Wang, R. Shewmon, and I. L. Chuang, *Phys. Rev. Lett.* **101**, 180602 (2008).

²⁷I. P. Levkivskyi and E. V. Sukhorukov, *Phys. Rev. Lett.* **103**, 036801 (2009).

²⁸D. B. Gutman, Y. Gefen, and A. D. Mirlin, *Phys. Rev. B* **81**, 085436 (2010).

- ²⁹C. Chamon, A. W. W. Ludwig, and C. Nayak, *Phys. Rev. B* **60**, 2239 (1999).
- ³⁰P. Nozières and F. Gallet, *J. Phys. (France)* **48**, 353 (1987).
- ³¹H. J. F. Knops and L. W. J. den Ouden, *Physica A* **103**, 597 (1980).
- ³²S. A. Bulgadaev, *Zh. Eksp. Teor. Fiz.* **39**, 264 (1984).
- ³³M. P. A. Fisher and W. Zwerger, *Phys. Rev. B* **32**, 6190 (1985).
- ³⁴A. Schmid, *Phys. Rev. Lett.* **51**, 1506 (1983).
- ³⁵S. Chakravarty, *Phys. Rev. Lett.* **49**, 681 (1982).
- ³⁶G.-L. Ingold and Y. V. Nazarov, NATO ASI Series B **294**, 21 (1992).
- ³⁷M. A. Cazalilla, *Phys. Rev. Lett.* **97**, 156403 (2006).
- ³⁸A. Altland and B. D. Simons, *Condensed Matter Field Theory*, 1st ed. (Cambridge University Press, Cambridge, UK, 2006).